HHS Public Access

Author manuscript

Nat Microbiol. Author manuscript; available in PMC 2024 March 22.

Published in final edited form as:

Nat Microbiol. 2024 January ; 9(1): 95–107. doi:10.1038/s41564-023-01546-0.

Candida albicans extracellular vesicles trigger type I IFN signalling via cGAS and STING

Hannah Brown Harding[1,2], **Geneva N. Kwaku**[1], **Christopher M. Reardon**[1], **Nida S. Khan**[1], **Daniel Zamith-Miranda**[3,4], **Robert Zarnowski**[5,6], **Jenny M. Tam**[7], **Collins K. Bohaen**[8], **Lauren Richey**[9], **Kenta Mosallanejad**[10], **Arianne J. Crossen**[1], **Jennifer L. Reedy**[1,2], **Rebecca A. Ward**[1], **Diego A. Vargas-Blanco**[1,2], **Kyle J. Basham**[1], **Roby P. Bhattacharyya**[1,2,11], **Jeniel E. Nett**[5,6], **Michael K. Mansour**[1,2], **Frank L. van de Veerdonk**[8], **Vinod Kumar**[8,12,13], **Jonathan C. Kagan**[10], **David R. Andes**[5,6], **Joshua D. Nosanchuk**[3,4], **Jatin M. Vyas**[1,2,11,✉]

[1]Division of Infectious Diseases, Department of Medicine, Massachusetts General Hospital, Boston, MA, USA.

[2]Department of Medicine, Harvard Medical School, Boston, MA, USA.

[3]Department of Microbiology and Immunology, Albert Einstein College of Medicine, Bronx, NY, USA.

[4]Division of Infectious Diseases, Department of Medicine, Albert Einstein College of Medicine, Bronx, NY, USA.

[5]Department of Medicine, University of Wisconsin-Madison, Madison, WI, USA.

[6]Department of Microbiology and Immunology, University of Wisconsin Madison, Madison, WI, USA.

[7]Wyss Institute for Biologically Inspired Engineering, Harvard University, Boston, MA, USA.

[8]Department of Internal Medicine and Radboud Center for Infectious Diseases, Radboud University Medical Center, Nijmegen, the Netherlands.

[9]Tufts Comparative Medicine Services, Tufts University, Boston, MA, USA.

✉**Correspondence and requests for materials** should be addressed to Jatin M. Vyas. jvyas@mgh.harvard.edu.

Author contributions

Conceptualization: H.B.H. and J.M.V. Investigation: H.B.H., G.K., C.M.R., N.S.K., D.Z.M., R.Z., J.M.T., A.C., C.K.B., L.R., V.K., D.A.V.-B., K.J.B. and J.L.R. Writing: H.B.H., R.A.W. and J.V. Paper review and revision: all authors. Resources: K.M., R.B., J.E.N., F.L.v.d.V., L.R., J.C.K., D.R.A. and J.D.N.

Ethical approval and consent to participate

The 500FG cohort was approved by the Arnhem-Nijmegen Medical Ethical Committee (500FG:NL42561.091.12) and performed in accordance with the Declaration of Helsinki. All individuals gave written informed consent to donate venous peripheral blood for research.

Competing interests

The authors declare no competing interests.

Additional information

Extended data is available for this paper at https://doi.org/10.1038/s41564-023-01546-0.

Supplementary information The online version contains supplementary material available at https://doi.org/10.1038/s41564-023-01546-0.

Peer review information *Nature Microbiology* thanks Tobias Hohl, Guilhem Janbon, Mairi Noverr and the other, anonymous, reviewer(s) for their contribution to the peer review of this work.

[10]Division of Gastroenterology, Boston Children's Hospital, Harvard Medical School, Boston, MA, USA.

[11]Broad Institute of MIT and Harvard, Cambridge, MA, USA.

[12]University Medical Center Groningen, Department of Genetics, University of Groningen, Groningen, the Netherlands.

[13]Nitte University Centre for Science Education and Research, Medical Sciences Complex, Mangaluru, India.

Abstract

The host type I interferon (IFN) pathway is a major signature of inflammation induced by the human fungal pathogen, *Candida albicans*. However, the molecular mechanism for activating this pathway in the host defence against *C. albicans* remains unknown. Here we reveal that mice lacking cyclic GMP–AMP synthase (cGAS)–stimulator of IFN genes (STING) pathway components had improved survival following an intravenous challenge by *C. albicans*. Biofilm-associated *C. albicans* DNA packaged in extracellular vesicles triggers the cGAS–STING pathway as determined by induction of interferon-stimulated genes, IFNβ production, and phosphorylation of IFN regulatory factor 3 and TANK-binding kinase 1. Extracellular vesicle-induced activation of type I IFNs was independent of the Dectin-1/Card9 pathway and did not require toll-like receptor 9. Single nucleotide polymorphisms in cGAS and STING potently altered inflammatory cytokine production in human monocytes challenged by *C. albicans*. These studies provide insights into the early innate immune response induced by a clinically significant fungal pathogen.

Candida albicans bloodstream infections are a dreaded complication of modern medicine, leading to mortality rates exceeding 50%[1,2]. Treatment of this deadly infection is limited due to the eukaryotic nature of this pathogen and requirement of sterilizing immunity, coupled with a lack of mechanistic understanding of how *C. albicans* communicates with the host immune system. Transcriptomic analysis in human peripheral blood mononuclear cells (PBMCs) identified the type I interferon (IFN) signature profile in response to *C. albicans* infections[3]. In addition to bloodstream infections, mucosal infection models demonstrate dynamic IFN responses using multiple *Candida* species[4]. Known IFN-stimulated genes (ISGs), MDA5, and the IFN receptor, IFNAR, are involved in the immune response to *C. albicans*[5–7]. The concept that *C. albicans* triggers a potent and seemingly antiviral-type IFN response is novel, and the mechanism of activation, including the full repertoire of fungal ligands involved, has not been discovered. The stimulator of IFN genes (STING) pathway is a major IFN-producing pathway known to respond to microbial pathogens[8,9]. Recently, STING has been shown to bind to Src to inhibit Syk-mediated signalling in dendritic cells challenged with *C. albicans*[10]. STING pathway activation can also occur upon cyclic GMP–AMP synthase (cGAS) sensing of double-stranded DNA in the cytosol[11–18], triggering a signalling cascade that activates the IFN regulatory factor 3 (IRF3) transcription factor to transcribe early ISGs and type I IFNs (IFNβ and IFNα)[19].

C. albicans and other pathogenic fungi secrete extracellular vesicles (EVs) that contain effector molecules, virulence factors, surface proteins and nucleic acids in order to transfer

information and facilitate crosstalk between fungal cells[20–24]. *C. albicans* EVs present themselves as strong candidates for the stimulating agent of the STING pathway as they contain nucleic acids, elicit a pro-inflammatory immune response, are major constituents of biofilms (BFs) and fungal masses, and can be internalized by immune cells[23,24]. EVs containing DNA secreted from the gut microbiota are known to activate type I IFN and trigger peripheral cGAS–STING[25]. We hypothesized that *C. albicans* EVs contain the ligand that triggers cGAS- and STING-dependent type I IFN signalling in the cytoplasm of macrophages before the host cell physically encounters a fungal organism. We further hypothesized that host cells, like macrophages, hijack fungal EVs to rewire and prime for an impending pathogen challenge.

In this Article, we reveal a strong connection between the STING innate immune signalling pathway in macrophages and *C. albicans*. Together, the data reveal a model of host cell re-programming that occurs as innate immune cells encounter *C. albicans* EVs before pathogen engagement. These findings are the first to present a mechanism of cGAS–STING pathway activation in macrophages by a fungal pathogen and identify a role for EVs in priming of host cells for an impending infection.

Results

cGAS and STING deletion improves survival

To determine if the STING pathway is critical for the host defence against *C. albicans*, we challenged wild-type (WT), *cGas*$^{-/-}$ and *Sting*$^{-/-}$ mice with intravenous *C. albicans* using an in vivo model of systemic candidiasis. Mice were infected with a lethal dose of *C. albicans* (SC5314), and survival was measured for >3 weeks (cGAS$^{-/-}$, 28 days; Fig. 1a, and STING$^{-/-}$, 22 days; Fig. 1b). In both experiments, *C. albicans* infection of WT mice resulted in 100% mortality before the conclusion of the experiment, whereas 60% of the mice lacking either cGAS or STING survived. These data demonstrate that mice lacking either of these integral components of the STING pathway had increased resistance to a lethal dose of *C. albicans*.

STING facilitates renal fungal clearance

To examine the impact of STING pathway activation by *C. albicans*, we investigated the ability of WT and *Sting*$^{-/-}$ mice to clear this pathogen by assessing fungal burden in the kidneys. We observed that *C. albicans*-infected *Sting*$^{-/-}$ mice had higher fungal kidney burden compared with WT mice. This high fungal kidney burden persists up to day 28 in *Sting*$^{-/-}$ mice that survived the course of infection (Fig. 1c). While some fungal organisms were detectable in other organs (liver, spleen and brain), this difference in fungal burden was exclusive to the kidneys of the surviving *Sting*$^{-/-}$ mice (Extended Data Fig. 1a). WT and *Sting*$^{-/-}$ mice displayed similar blood urea nitrogen (BUN) and creatinine levels over the course of infection, indicating that altered kidney function does not explain the enhanced survival of the *Sting*$^{-/-}$ mice (Extended Data Fig. 1b,c). The increased presence of fungal organisms in *Sting*$^{-/-}$ mice compared with WT was confirmed by Grocott's methenamine silver (GMS) staining of kidney tissue to visualize *C. albicans* (Fig. 1d and Extended Data Fig. 1h). Kidney sections from day 5 of WT and *Sting*$^{-/-}$ mice infected with *C.*

albicans were also stained with haematoxylin and eosin (H&E) to assess immune cell infiltration. While the overall number of immune cells appeared similar between the two groups, we did observe altered organization of the immune infiltration with severe abscesses in the medulla of WT kidneys, but not in the *Sting*$^{-/-}$ kidneys (Fig. 1d). To complement the histology, quantification of immune cell infiltrate in the kidneys was performed at day 5 post-infection using a multi-parametric flow-based immunophenotyping assay and subsequent gating strategy to identify immune cell populations (Extended Data Fig. 1d)[26,27]. We observed similar immune cell recruitment in the WT and *Sting*$^{-/-}$ kidneys (Extended Data Fig. 1e,f). In addition to the dramatic differences in immune cell localization in the kidneys, we observed that the effector functions of these cells differed in their ability to induce a known downstream output of the STING pathway, namely viperin (Extended Data Fig. 1g).

To further dissect the role of an active STING pathway in innate immune cells clearance of *C. albicans*, we tested fungal metabolic activity as a readout for viability following a 2 h co-culture with WT macrophages or macrophages lacking either cGAS or STING. We observed a significant increase in fungal cell death in the WT macrophage co-culture (Fig. 1e). Regardless of effector to target ratio, *cGas*$^{-/-}$ and *Sting*$^{-/-}$ macrophages killed *C. albicans* less effectively indicating a critical role for the STING pathway in fungal clearance. These paired in vivo and in vitro findings reveal an integral role for the STING pathway in reducing *C. albicans* burden during infection.

C. albicans EVs trigger the STING pathway

The critical role for cGAS and STING in responding to *C. albicans* suggested that fungal DNA activates the cytosolic sensor, cGAS. A known source of fungal nucleic acids is the extra-organismal content of EVs[22,23]; hence, we examined the role of *C. albicans* EVs as the source of the DNA ligand for STING pathway activation. Induction of viperin, one of the well-studied ISGs, and IFNβ secretion was used as a model of activation of the cGAS–STING pathway and assessed in WT, *cGas*$^{-/-}$ and *Sting*$^{-/-}$ macrophages following a 6-h stimulation with *C. albicans* EVs[13,28]. As ergosterol is a major constituent of the lipid bilayer of fungal EVs, we included an ergosterol only control[20]. We observed a significant increase in both viperin and IFNβ levels in WT macrophages stimulated with EVs. We did not see this significant increase in *cGas*$^{-/-}$ and *Sting*$^{-/-}$ macrophages (Fig. 2a,b). Importantly, both WT and *cGas*$^{-/-}$ macrophages produced high levels of IFNβ when stimulated with cGAMP (Fig. 2b), a downstream secondary messenger molecule produced when cGAS binds to DNA[13]. EVs from other *Candida* species, including *Candida auris*, also activated the STING pathway, as there was a significant increase in viperin and IFNβ levels in stimulated WT macrophages (Extended Data Fig. 2a,b). *C. auris* EVs grown from an agar plate, although smaller in size than *C. albicans* EVs grown in the same way, induced viperin and IFNβ to similar levels (Extended Data Fig. 2a–c).

To assess the contribution of other fungal recognition receptors in the response to *C. albicans* EVs including toll-like receptor (TLR)9, Dectin-1 and caspase recruitment domain-containing protein (CARD)9[29–31], we stimulated *Tlr9*$^{-/-}$, *Dectin1*$^{-/-}$ and *Card9*$^{-/-}$ macrophages with *C. albicans* EVs and measured viperin and IFNβ. We observed a

significant increase in both viperin and IFNβ compared with the phosphate-buffered saline (PBS) control indicating that TLR9, Dectin-1 and CARD9 are not needed to facilitate this signalling response (Extended Data Fig. 2d,e).

We next assessed the ability for EVs extracted from different sources to induce the STING pathway. We identified the same cGAS- and STING-dependent viperin and IFNβ induction when macrophages were stimulated with increasing concentrations of EVs collected from *C. albicans* biofilms (BF EVs) grown for 48 h and to a lesser extent in EVs collected from *C. albicans* yeast (planktonic) (Fig. 2c,d). Importantly, we also observed that both viperin and IFNβ production in response to BF EVs was dose dependent (Extended Data Fig. 2f,g). *C. albicans* BF EVs are, on average, smaller than EVs prepped from agar plates or planktonic culture (Extended Data Fig. 2c); however, the pathway activation they induce remains strong.

Due to the robust effect of BF EVs on pathway activation, we investigated the cellular changes occurring in response to macrophage internalization of EVs. cGAS localization is a dynamic and reactive process such that it translocates intracellularly from the nucleus to the cytosol to sense cytosolic DNA[32–34]. In an unstimulated macrophage, cGAS is tethered tightly to the nuclear membrane to prevent autoreactivity[34]. However, the localization of this DNA sensor changes in response to infection and stimulation[35]. To assess whether *C. albicans* BF EV stimulation alters cGAS subcellular localization within macrophages, we labelled the lipid membranes of EVs with DiI and co-cultured them with WT macrophages expressing cGAS–green fluorescent protein (GFP). We observed a significant increase in non-nuclear localization patterns in macrophages with internalized EVs (Fig. 2e,f). We did not observe this phenotype when treating with a PBS sample exposed to DiI labelling (Extended Data Fig. 3). These data indicate that *C. albicans* EV stimulation results in the activation of the STING pathway and dynamic subcellular redistribution of cGAS within macrophages.

C. albicans BF DNA activates the STING pathway

Since the STING pathway senses foreign double-stranded DNA, we characterized *C. albicans* EV DNA. First, we assessed whether DNA was present on the exterior surface of EVs by treating with Benzonase (DNase)[36] before stimulation of WT macrophages. When comparing Benzonase-treated EVs with untreated EVs, viperin was not differentially induced indicating that the stimulating DNA is not freely exposed (Extended Data Fig. 4a). Next, we extracted DNA from EVs and transfected it into WT macrophages. Even at low concentrations, EV DNA was sufficient to induce viperin, supporting the hypothesis that *C. albicans* EVs contain DNA that triggers STING pathway activation (Extended Data Fig. 4a). To ensure that the DNA packaged within *C. albicans* EVs was indeed fungal, we sequenced DNA extracted from BF EVs. We identified the eight most abundant genes in this EV DNA (Supplementary Table 1). Importantly, these genes are *C. albicans* specific and none has murine or human orthologues, which provides unambiguous insight into the origin of this DNA.

Approximately 5% of *C. albicans* BFs is composed of extracellular DNA hypothesized to be packaged in EVs[37,38]. Therefore, we extracted DNA from *C. albicans* BFs (BF DNA) grown

for 48 h, 72 h and 96 h, then transfected concentrated BF DNA into WT macrophages for 6 h. We observed robust viperin induction and IFNβ production regardless of BF growth time (Extended Data Fig. 4b,c). Since the 72 h timepoint demonstrated the most robust induction, we conducted all subsequent BF DNA stimulations with BF DNA grown for 72 h.

We next assessed the transfection and DNA-dependency of viperin and IFNβ induction. We stimulated WT macrophages with cGAMP (transfected into cells or not), BF DNA (transfected or not) or BF DNA treated with Benzonase before transfection. Only cGAMP and transfected BF DNA induced viperin and IFNβ (Fig. 2g,h). To determine whether this induction was dependent on cGAS and STING, we assessed viperin and IFNβ levels in WT, *cGas*$^{-/-}$ and *Sting*$^{-/-}$ macrophages following transfection with *C. albicans* BF DNA. As with *C. albicans* EVs, we observed significant increases in viperin and IFNβ in WT macrophages stimulated with BF DNA and cGAMP, whereas the *cGas*$^{-/-}$ and *Sting*$^{-/-}$ macrophages failed to produce either output (Fig. 2i). Furthermore, BF DNA stimulation of WT macrophages resulted in phosphorylated TANK-binding kinase (TBK1) and IRF3 indicating that downstream elements of the STING pathway are activated in response to BF DNA. *cGas*$^{-/-}$ and *Sting*$^{-/-}$ macrophages failed to induce phosphorylation of either protein, as well as IFNβ production, indicating that the BF DNA pathway activation is cGAS- and STING-dependent (Fig. 2h and Extended Data Fig. 4d,e). Moreover, we observed significant increases in viperin and IFNβ levels in *Tlr9*$^{-/-}$, *Dectin1*$^{-/-}$ and *Card9*$^{-/-}$ macrophages stimulated with BF DNA, indicating that these proteins are dispensable for activation of this pathway (Extended Data Fig. 4d,e). Finally, pre-treatment of WT macrophages with Dynasore, an inhibitor of dynamin-dependent endocytosis, resulted in a complete ablation of viperin induction in cells, subsequently stimulated with both *C. albicans* EVs and transfected BF DNA (Fig. 2j). These data support a model where endocytosed EVs deploy their DNA cargo into the cytoplasm where it is then sensed by cGAS–STING.

Due to the potential for pleiotropic effects of a full knockout cell line, we treated WT macrophages with increasing concentrations of the STING inhibitor H-151[39,40]. Similarly to the *Sting*$^{-/-}$ macrophages, this specific drug treatment reduced levels of viperin, phospho-TBK1, and phospho-IRF3 in cells stimulated with cGAMP, BF DNA and EVs, but did not reveal as significant of a reduction in LPS-stimulated cells, as LPS triggers STING-independent IFN signalling (Extended Data Fig. 4f,g).

Host response to *C. albicans* EVs and BF DNA

The ability of both *C. albicans* EVs and BF DNA to elicit induction of known ISGs in a cGAS- and STING-dependent manner prompted us to assess the extent of the ISG induction. We stimulated WT, *cGas*$^{-/-}$ and *Sting*$^{-/-}$ macrophages with PBS and EVs for 6 h, extracted RNA from these immune cells and assessed the expression of 772 host response genes, which included 440 known ISGs. Using nCounter, we identified 73 genes induced by EVs as compared with the PBS control, including numerous early ISGs (that is, *IFIT1*, *RSAD2* (viperin), *OASL1*, ISG15, *IFIH1*/MDA5, *DHX58* and *DDX58*/*RIG-I*) (Fig. 3a and Supplementary Table 2a). Transcripts from early ISGs are known to be induced within 3–6 h of infection, independent of IFNβ production[41]. In parallel, RNA from macrophages stimulated with Lipofectamine reagents alone or with transfected BF DNA was analysed

against the same host response panel. BF DNA specifically induced 18 genes in WT macrophages (Supplementary Table 2b), including the early ISGs: IFIT1, *Rsad2*RSAD2, OASL1, ISG15 and DDX58. Genes induced by EVs and BF DNA in WT macrophages overlapped greatly as demonstrated by the 13 shared genes, including early ISGs (Fig. 3a and Supplementary Table 2c).

To determine if these 13 shared inflammatory genes are induced in a cGAS- and STING-dependent manner, we examined their expression levels in response to EVs and BF DNA in *cGas*$^{-/-}$ and *Sting*$^{-/-}$ macrophages. *RSAD2*, *IFIT3* and *ISG15* are highly induced by both stimulants in WT macrophages, but not in macrophages lacking cGAS or STING (Fig. 3b and Supplementary Table 2d). *CXCL10* and *DDX58* are induced by EVs, but not in a cGAS- and STING-dependent manner (Fig. 3b). All genes induced by BF DNA were upregulated in WT macrophages, but not in *cGas*$^{-/-}$ and *Sting*$^{-/-}$ (Fig. 3b). To validate our findings, we performed quantitative reverse transcription polymerase chain reaction (RT–qPCR) of *RSAD2*, *OASL* and *IFIT3* induced by both EVs and BF DNA, which demonstrated potent upregulation of transcripts in a cGAS- and STING-dependent manner (Fig. 3c–e). Genes upregulated by EVs, regardless of cGAS and STING activity, included genes involved in the inflammasome pathway (for example, *NLRP3* and *CASP4*) (Supplementary Table 2a,e,g), which is known to respond to cytosolic and double-stranded DNA[42–44]. Furthermore, *IL1B*, *CXCL2*, *Il1F6*, *LCP2*, *IRF9*, *CSF2RB* and *ADAR* were induced by EVs in the *cGas*$^{-/-}$ and *Sting*$^{-/-}$ macrophages, but not in WT, suggesting activation of compensatory DNA sensing pathways not normally triggered by EVs (Supplementary Table 2).

cGAS and STING polymorphisms in human monocytes

To determine if cGAS and STING are relevant in human immunity to *C. albicans* infection, we investigated single nucleotide polymorphisms (SNPs) of both cGAS and STING in human monocytes exposed to the fungal pathogen and assessed whether these SNPs led to changes in cytokine levels. We probed a previously published large cohort of patients in which PBMCs were isolated from healthy volunteers and stimulated with *C. albicans*. In the published study, the authors found that genetic variation in type I IFN pathway genes (IRF1 and STATa) correlated with *C. albicans*-induced release of the following seven cytokines: tumour necrosis factor (TNF)α, interleukin (IL)1β, IL8, IL6, IL10, IFNγ and IL17[3]. We queried this existing database for variations in the genetic regions encoding cGAS and STING and correlations with production on the two cytokines known to be produced by STING-dependent activation of the nuclear factor κB transcription factor: IL6 and TNFα[8,45]. Based on quantitative trait loci mapping, we identified that SNPs in the regions on chromosomes 5 and 6 (containing cGAS and STING, respectively) correlate with changes in production of TNF and IL6 (Fig. 4 and Extended Data Fig. 5). Specifically, we identified a significant SNP in genetic region MB21D1 (*cGAS*) with an associated genotype (GG) with decreased levels of cGAS (as evident by the negative *z*-score in Extended Data Fig. 5e), which correlates with decreased *C. albicans*-induced TNFα and IL6 (Fig. 4a,b). We also identified a significant SNP in genetic region TMEM173 (*STING*). This SNP has an associated genotype (CC) leading to increased levels of STING (as evident by the positive *z*-score in Extended Data Fig. 5e), which correlates with decreased TNFα and increased IL6 (Fig. 4c,d). We assessed whether these cGAS and STING-dependent changes

in TNFα levels exist in our murine macrophage model when exposed to *C. albicans*. Indeed, TNF production is highly induced in murine macrophages lacking either cGAS or STING as compared with WT macrophages (Extended Data Fig. 5f). These data provide direct evidence that changes in expression in cGAS and STING alter cytokine levels secreted by both human monocytes and murine macrophages challenged by *C. albicans*.

Discussion

We demonstrate a novel connection between the innate immune STING pathway and EVs produced by the fungal pathogen, *C. albicans*. Specifically, we have identified that *C. albicans* activates the STING pathway in macrophages via EVs delivering fungal DNA to the cytosol of macrophages and triggering engagement of cGAS and initiation of downstream signalling. This signalling triggers the expression of many early ISGs, IFNβ and other innate immune processes historically associated with viral and bacterial infections[8,11,14,16–18]. Furthermore, we identified that activation of this pathway clears the fungal infection, but at the detriment to the host. Importantly, STING activation is relevant in both mouse and human models of candidaemia as demonstrated through in vivo studies and SNP analysis, respectively. While type I IFNs had been implicated previously in candidemia in humans, little was known about the mechanism of this activation or the immune pathways involved[3,4,6,46]. We have now identified a major innate immune pathway involved in this type I IFN response and further characterized how *C. albicans* interacts with its components.

EVs are integral in fungal biology as they assist in pathogen intracellular communication to develop BFs and coordinate community dynamics[25,47–49]. *C. albicans* and other EV-producing microbial organisms use EVs to package important signalling and effector molecules to communicate with the surrounding community. These signals, packaged as cargo in these lipid bilayer membrane vesicles, can respond to changes in microenvironments by providing drug resistance, altering cell adhesion and disseminations properties, and enhancing BF matrix production[20,47]. Mammalian cells also make EVs and are able to recognize and internalize them for their own community organization[50–55]. This coordination can be useful for general growth and development purposes of healthy cells, but can also be usurped by tumour cells to prioritize proliferation of surrounding cancerous cells and metastasis[56–58]. Macrophages endocytose and respond to microbial EVs[20,59]. Our data support this by revealing a novel form of immune cell surveillance, in which macrophages internalize fungal EVs and co-opt them for the purposes of rewiring innate immunity to generate a robust type I IFN response, which can prime phagocytic cells to kill engulfed pathogens more efficiently. Specifically, we identified the STING pathway as integral to this immune response to DNA packaged inside *C. albicans* EVs, which might be linked to the known role of the STING pathway in macrophage metabolic re-programming following infection[60]. For example, STING pathway activation via *Brucella abortis* infection increases intracellular succinate levels and shifts glycolytic profiles of inflammatory macrophages[60]. Fungal EVs could similarly trigger this glycolytic switch to quickly clear invading fungal pathogen. It is also known that the ISG response promotes the phagocytic activity and microbial killing capacity of macrophages via increased acidity of the phagolysosome[61]. Therefore, EVs might be signalling to the macrophage of an impending viable microbial organism and triggering a drop in lysosomal pH. We

demonstrated that following both EV and BF DNA stimulation, the type I IFN response is upregulated and that this has functional consequences for both the host cell and the live microbe. Future studies will investigate the extent to which this re-programming affects immune cell function.

We demonstrated that *C. albicans* and *C. auris* EVs rewire cells towards a type I IFN response. Historically, fungal recognition has been focused on C-type lectin receptors, TLRs, RIG-I-like receptors and the inflammasome sensing various cell wall epitopes[62–67]. These receptors, while highly influential of disease outcome, were not explicitly linked to the type I IFN response. Studies have since observed the induction of a type I IFN signature profile in response to *C. albicans* in human PBMCs[3] and dendritic cells[5] and identified type I IFN-induced ISGs as essential for the host response to candidemia[7,46,68]. Recently, a study demonstrated that *Candida* spp. elicit a mitochondrial-associated type I IFN response in vaginal epithelial cells[4]. Furthermore, clinical studies have found increased IFNα and IFNβ levels in the vaginal fluid of patients suffering from vulvovaginal candidiasis[69]. One other study assessing the ability for nucleic acids from yeast to induce a type I IFN response identified that yeast DNA and RNA activate IFNβ responses in dendritic cells via signalling through TLRs, but did not observe this response in macrophages nor did they investigate the potential role of the STING pathway[70].

Our studies enhance our understanding of the *Candida*-induced type I IFN response by identifying the cGAS–STING pathway as integral for this innate immune response. We further identified that the source of the *C. albicans* nucleic acids sensed by cGAS is not from phagocytosed yeast, but from *C. albicans* EVs delivering double-stranded fungal DNA into the cytosol following endocytosis. While the exact mechanism is unknown, *Aspergillus fumigatus* also activates the STING pathway in a keratitis model of infection[71]. Perhaps *A. fumigatus* EVs function similarly to deliver DNA cytosolically[72,73]. *A. fumigatus* has also been shown to activate a coordinated type I and III IFN response in the lung, warranting future studies to elucidate the ability of EVs from other pathogenic fungi to activate this signalling pathway[74,75]. Additionally, investigating the ability for neurotropic pathogenic fungi such as *Cryptococcus neoformans* and *Coccidioides posadasii* to make EVs that can activate the STING pathway is merited, as there is evidence that microglia can activate the STING pathway[76]. Expanding our studies past *Candida* species would be an exciting next step in elucidating the intimate relationship between fungal pathogens and the type I IFN response.

We have demonstrated a novel connection between *C. albicans* and the STING pathway and revealed fungal DNA packaged in released EVs as the mechanism of activation. Furthermore, we identified the functional consequences of this signalling in both mouse and human models, highlighting the physiologic relevancy of these findings. Overall, the results presented here have significantly enhanced our understanding of the type I IFN response initiated by a human fungal pathogen.

Methods

In vivo studies

In vivo infection studies were carried out as previously described[77]. Briefly, *C. albicans* (WT strain SC5314) was grown in yeast extract peptone dextrose (YPD) medium for 16 h at 30 °C in a shaker incubator at 250 rpm. *C. albicans* was washed and resuspended at a concentration (500,000 yeast ml^{-1}) in ice-cold PBS. WT C57BL/6 (JAX #000664), $cGAS^{-/-}$ C57BL/6 (a gift from the Stetson Laboratory[78]) and $Sting^{-/-}$ B6(Cg) (JAX no. 025805) mice were injected intravenously into the lateral tail vein with *C. albicans* (100,000 or 150,000 yeast). We chose to use this knockout mice strain instead of goldenticket, which carries a missense mutant allele of the Sting gene (JAX no. 017537), which theoretically may carry residual function. Following the *C. albicans* challenge, mice were monitored twice daily for morbidity and mortality for up to 28 days. Mice displaying pre-specified criteria for distress (inability to feed or drink, laboured breathing, ruffled and/or matted fur, decreased activity, hunched posture and shivering) were euthanized by CO_2 asphyxiation. All mouse experiments were approved by the MGH Institutional Animal Care and Use Committee under protocol no. 2008N00078.

Organ burden quantification, kidney BUN and creatinine

Organs (kidneys, livers, spleens and brains) were collected from infected WT and $Sting^{-/-}$ mice at different points during the infection. Organ weights were obtained, and each organ was homogenized using a sterilized and PBS-washed Dounce homogenizer for 30 s at a time until the organs formed a homogenate. Organ suspensions were then diluted in 1 ml of PBS and serially diluted. Then 100 µl of each dilution was plated onto YPD agar and allowed to grow at 30 °C for 48 h. Colony forming units were calculated by the following formula: (number of colonies × dilution factor × 10)/organ (g) ($n = 8$ for WT and 14 for $Sting^{-/-}$ for each timepoint in Fig. 1c and $n = 4$ for WT and 4 for $Sting^{-/-}$ for each time point in Extended Data Fig. 5a).

Kidney BUN and creatinine levels were measured from serum of infected and uninfected WT and $Sting^{-/-}$ mice. Whole blood was collected from mice posthumously and left to clot for 45 minutes at room temperature. Blood was then spun at 12,000*g* for 10 min at 4 °C. Serum was then separated, frozen and given to the Clinical Pathology Laboratory in the Center for Comparative Medicine at Massachusetts General Hospital for analysis.

Immunophenotyping by flow cytometry and histopathology

WT and $Sting^{-/-}$ mice ($n = 6$) were infected with 150,000 *C. albicans* yeast intravenously. Uninfected control mice were also processed for analysis. Mice were euthanized at 5 days post-infection, and immunophenotyping was performed as previously described[26,27]. Briefly, kidneys were excised, placed into digestion solution (collagenase type IV and 100 U DNase I in 100 ml Roswell Park Memorial Institute (RPMI) 1640 medium), finely minced using scissors and incubated for 1 h with shaking at 37 °C. After 1 h, 800 ml of 0.5 M ethylenediaminetetraacetic acid was added to each sample to stop the collagenase activity. Kidney samples were passed through a 70 mM filter, pelleted, resuspended in a 40% Percoll-RPMI solution and under-layered with a 67% Percoll–RPMI solution. Samples were

centrifuged at 650*g* for 20 min and leukocytes were collected at the interface between layers and washed twice with flow cytometry (FACS) buffer (PBS with 2% foetal bovine serum (FBS)). Cells were then treated with ammonium–chloride–potassium buffer to lyse the red blood cells for 5 min at room temperature (RT) and spun at 1200 rpm. All cells were stained for flow cytometry analysis. Fc block (anti-mouse CD16/CD32, Thermo Fisher Scientific, 14–0161–85) was added to cells at 1:100 dilution and incubated at RT for 15 min. Cells were then labelled with a mixture of the following fluorophore-conjugated antibodies for 1 h at 4 °C (all antibodies are from Biolegend, unless otherwise noted): anti-CD45 BV605 (Biolegend, 103139), anti-CD90.2 BV786 (Biolegend, 105331), anti-CD19 PE-Dazzle (Biolegend, 115553) and anti-Ly6G AF 488 (Biolegend, 127625). Cells were washed with FACS buffer, and 7-aminoactinomycin D (Stem Cell Technologies, 75001.1) was added for live-dead cell staining. Flow cytometry was performed using BD FACSCelesta and analysis was performed using FlowJo 10 software (BD). Quantification was performed in GraphPad Prism9 and FlowJo 10.9.0.

For histopathology, kidney tissue was collected and fixed in 10% neutral buffered formalin, trimmed, processed routinely, embedded in paraffin, sectioned (5 μm) and stained with H&E and GMS. Histology was performed by Tufts Comparative Medicine Services at Tufts University. Histopathology was evaluated by a board-certified veterinary pathologist. Images were obtained using 10× magnification.

Cell culture and macrophage cell line generation

All immortalized bone marrow-derived macrophages were cultured in complete Dulbecco's modified eagle medium (cDMEM) (supplemented with 10% FBS, penicillin and streptomycin (Pen+Strep), L-glutamine and 1 M hydroxyethylpiperazine ethane sulfonic acid at 37 °C in 5% CO_2. For passage, macrophages were washed with PBS and lifted with 0.25% trypsin diluted at 1:10. The following cell lines were used: WT immortalized bone marrow-derived macrophages gifted by Douglas Golenbock (University of Massachusetts Medical School), *cGas*$^{-/-}$ and *Sting*$^{-/-}$ macrophages were generated as previously described[79], *Dectin-1*$^{-/-}$ immortalized macrophages were a gift from Gordon Brown (University of Aberdeen) and Stuart Levitz (University of Massachusetts Medical School), *Tlr9*$^{-/-}$ macrophages were generated as previously described[80], *Card9*$^{-/-}$ macrophages were a gift from Ramnik Xavier (Harvard Medical School), and cGAS–GFP expressing macrophages were generated as previously described[35]. All macrophage lines were immortalized from C57BL/6 mice.

PrestoBlue killing assay

The PrestoBlue assay was used to measure fungal viability of *C. albicans* as previously described[72]. WT, *cGas*$^{-/-}$ and *Sting*$^{-/-}$ macrophages were plated in triplicate in a 96-well plate at a density of 1×10^4 cells per well. Following an overnight incubation, the cells were stimulated with either PBS or live *C. albicans* for 2 h at 37 °C and 5% CO_2. *C. albicans* only controls were also plated to determine the uninhibited rate of growth for end-point comparison. The ratio of fungal cell to macrophage was changed to allow for further interpretation of killing dynamics (1:1, 1:5 and 5:1). Plate was spun down at 1,200 rpm for 1 min before incubation to ensure contact of cells with fungi. Cells were then lysed

with NP-40 to liberate phagocytosed yeast cells and placed on ice for 5 min. Fresh 3-(N-morpholino)propanesulfonic acid–RPMI pH 7 4 and PrestoBlue (Thermo Fisher Scientific, no. A13261) was added to each well and mixed thoroughly. The plate was then incubated at 37 ˚C for 10 min and then moved to 30 °C to incubate for 2 h in the dark. Fluorescence was measured using a SpectraMax i3× Multi-Mode Microplate Reader system (Molecular Devices) analysing the 560/590 nm wavelength one time. Percentage of live *C. albicans* compared with no macrophage control wells was determined using excel and statistical significance was assessed using GraphPad Prism9 software (GraphPad Software). $P < 0.05$ was considered significant.

EV isolation and purification from YPD agar lawns

Fungal EVs were isolated from *C. albicans* (SC5314) and *C. auris* (Biosample accession number SAMN05379624) as previously described[81]. Briefly, one colony of each fungus was inoculated in Sabouraud broth and incubated overnight at 30 °C under constant shaking. Yeast cells were transferred to YPD agar plates (~10^7per plate) and spread using glass beads. The plates were incubated at 30 °C for 48 h. The cell lawns were carefully scraped from the plates and transferred to conical tubes containing PBS. Cell suspensions were centrifuged at 1,500*g* and the resulting supernatant was centrifuged again at 5,000*g*. The supernatant was filtered through a 0.8 μm membrane and then ultracentrifuged at 150,000*g*. After discarding the supernatant, EVs were suspended in PBS, and the ergosterol concentration was quantified using the Amplex Red cholesterol assay kit (Thermo Fisher). EV suspensions were stored at 4 °C. EVs were further quantified using the NanoSight core facility at Massachusetts General Hospital.

Isolation and characterization of *C. albicans* EVs from BF and planktonic culture

EVs were isolated from both planktonic and BF cultures from *C. albicans* (WT strain SN250). A volume of 1-litre batches of planktonic cultures were grown in two Erlenmeyer flasks at 30 °C at 200 rpm for 24 h and 48 h[24], whereas BF cultures were grown in the large-scale system employing polystyrene roller bottles at 37 °C at 4 rpm for 24 h and 48 h[82]. Planktonic culture supernatants were separated from cell biomass by centrifugation at 10,000*g for* 10 min at 4 °C and filter sterilized. BF culture media were carefully decanted, remaining suspended debris was removed by filtration through a paper filter and then filter-sterilized. Collected culture supernatants concentrated down to 25 ml using a Vivaflow 200 unit (Sartorius AG) equipped with a Hydrosart 30 kDa cutoff membrane. The samples were then centrifuged at 10,000*g* for 1 h at 4 °C to remove larger cellular/membrane-like particulates. The pellets were discarded, and the collected supernatants were next centrifuged in a Beckman Coulter Optima MAX-XP Ultracentrifuge equipped with an MLA-50 fixed rotor at 100,000*g* for 1.5 h at 4 °C. The resulting supernatants were subsequently discarded, whereas the pellets were resuspended in 5 ml of PBS (pH 7.2) and re-centrifuged in the ultracentrifuge utilizing an MLS-50 swinging bucket at 100,000*g* for 1 h at 4 °C. The collected EVs were then polished by flash size-exclusion chromatography on qEV/35 nm columns (Izon Science), filter sterilized and stored until further use at 4 °C[47].

Purified EVs were quantified using nanoparticle tracking analysis. EV samples were diluted in PBS to a final volume of 1 ml and pre-tested to obtain an ideal count of 30–100

particles per frame rate using a NanoSight NS300 system equipped with a sample assistant autosampler (Malvern). The following settings were applied: camera level was increased to 16 and camera gain to 2 until tested images were optimized and nanoparticles were distinctly visible without exceeding particle signal saturation. Each measurement consisted of five 1-min videos with a delay of 5 s between sample introduction and the start of the first measurement. For detection threshold analysis the counts were limited to 10–100 red crosses and no more than 5–7 blue crosses. Acquired data were analysed using the NanoSight Software NTA 3.4 Build 3.4.003. At least 1,000 events in total were tracked per sample to minimize data skewing based on single large particles[22].

Analysis of DNA in *C. albicans* EVs

DNA was extracted from the purified BF EVs using the MasterPure Yeast DNA Purification Kit (Lucigen). Briefly, EVs were resuspended in 300 µl of yeast cell lysis solution and incubated at 65 °C for 15 min. The samples were placed on ice for 5 min, and then 150 µl of milk protein concentrate protein precipitation reagent were added, vortex mixed for 10 s and centrifuged in a table-top microcentrifuge for 10 min. The supernatants were transferred to new Eppendorf tubes followed by addition of 500 µl of isopropanol and mixed thoroughly by inversion. DNA was collected by centrifugation in a table-top microcentrifuge for 10 min at the maximum speed. The pellets containing the environmental DNA were washed with 500 µl of 70% ethanol, dried briefly at 42 °C and placed in 50 µl of TE buffer. DNA concentration was determined using the Qubit dsDNA HS Assay Kit (Life Technologies). Libraries were then prepared according to the Celero PCR Workflow with Enzymatic Fragmentation (Tecan Genomics). Both quality and quantity of the finished libraries were assessed using an Agilent Tapestation (Agilent) and the Qubit dsDNA HS Assay Kit, respectively. Paired-end 150 bp sequencing was performed using the Illumina NovaSeq6000 (Illumina).

C. albicans DNA extraction from BF

WT *C. albicans* (SC5314) culture was grown overnight from a frozen culture and rotated in fresh YPD media at 30 °C. From the overnight culture, an inoculum of *C. albicans* was washed 3× with 1× PBS and diluted in cDMEM at 1×10^6 cells ml^{-1}. Inoculum was then plated to a 12-well tissue culture (TC)-treated plate at 1 ml per well in all 12 wells and spread to cover the bottom of each well. Plate was incubated at 37 °C with 5% CO_2 for 24 h, 48 h, 72 h or 96 h to grow BF before collection. BF DNA was extracted using the Norgen Biotek Biofilm DNA Isolation Kit (no. 62300) Briefly, using a cell lifter and sterile tweezers, 6 wells of the 12-well plate of BF were scraped and transferred to a microcentrifuge tube (200 mg wet weight). BFs were centrifuged at 20,000*g* for 1 min to collect the BF. Using tweezers, BF was transferred to a bead tube and protocol was followed per the kit instructions and the optional RNAse treatment was performed. Pure BF DNA was collected, measured by nanodrop and stored at −80 °C.

Immunoblot analysis

Macrophages were plated at a concentration of 1.5×10^5 cells ml^{-1} in a 12-well TC-treated plate and allowed to adhere overnight. For kidney homogenate experiments, kidneys were collected from mice at day 3 and 5 post-infection (left and right kidney were combined).

Kidneys were homogenized using a sterilized and PBS-washed Dounce homogenizer for 30 s at a time until the kidneys formed a homogenate. Kidney suspensions were then diluted 1:20 and treated as 'neat' lysates for subsequent immunoblot analysis. For Dynasore treatment experiments, macrophages were plated at a concentration of 1×10^5 cells ml^{-1} and allowed to adhere overnight. The following day, cells were washed with PBS and serum-free media were added to the cells with or without 100 μM Dynasore Hydrate (Sigma-Aldrich D7693). Cells were treated at 37 °C and 5% CO_2 for 30 min before subsequent stimulation. For H-151 treatment experiments, macrophages were plated at a concentration of 1×10^5 cells ml^{-1} and allowed to adhere overnight. The following day, macrophages were washed and 5 μM/0.5 μM H-151 (Selleck Chemicals S6652) was added to treated wells for 24 h before stimulation. Macrophages were either stimulated with PBS, EVs, LPS or transfected with cGAMP, *C. albicans* DNA from BF or EVs. Lipofectamine reagents alone containing DNA elution buffer were also used in some experiments as a negative control. Transfections were completed using the Lipofectamine 3000 reagents and protocol (Invitrogen L3000015). Lysates were collected following a 6 h incubation at 37 °C and 5% CO_2 using mammalian protein extraction reagent lysis buffer (Thermo Scientific, no. 78501) with sodium orthovanadate and protease inhibitors. Lysates were spun down (14,000*g* for 5 min at 4 °C), transferred to a fresh tube and subsequently mixed with 4× NuPage lithium dodecyl sulfate loading buffer and 10× NuPage reducing agent. Western blot assays were performed using a 4–12% NuPage gel, with 2-[N-morpholino]ethanesulfonic acid running buffer (NuPage gels, Thermo Fisher Scientific), and transferred to methanol activated polyvinylidene difluoride membrane (Perkin Elmer, Waltham, MA) using transfer buffer (0.025 M Tris, 0.192 M glycine and 20% methanol) and electrophoretic transfer at 100 V for 1 h. For detection of proteins, polyvinylidene difluoride membranes were blocked for 1 h at RT in 5% milk in PBS 0.01% Tween 20 (PBST). To detect the viperin (Sigma MABF106), TBK1 (Cell Signaling 3504) and IRF3 (Cell Signaling 4302) proteins, blots were incubated for 1 h at RT in PBST, 1% BSA and primary antibody (1:5,000, 1:1,000 and 1:1,000, respectively). To detect phosphorylated proteins, phospho-TBK1 (Cell Signaling D52C2) and phospho-IRF3 (Cell Signaling E6F7Q), blots were incubated overnight at 4 °C in tris-buffered saline with Tween 20 (TBST), 5% BSA and primary antibody (1:1,000). For phosphorylation specific probes, TBST (Cell Signaling 9997S) was used for all incubations and washes. Following incubation with primary antibody, blots were subsequently washed in either PBST or TBST 3× and incubated with secondary swine anti-rabbit horseradish peroxidase conjugated antibody at 1:2,000 (Agilent DAKO, P0399) or secondary peroxidase AffiniPure goat anti-mouse IgG (H and L) (Jackson ImmunoResearch) at 1:2,000 in 1% milk in PBST/TBST for 1 h at RT. To detect total protein via actin, blocked blots were incubated for 1 h at RT with simultaneous probing for actin (Cell Signaling 1:2,500) and secondary swine anti-rabbit horseradish peroxidase conjugated antibody. Membranes were washed 3× and then visualized using Western Lightning Plus ECL chemiluminescent substrate (Perkin Elmer) on Kodak BioMax XAR film (MilliporeSigma). Films were then scanned and processed using Adobe Illustrator. Any contrast adjustments were applied evenly to the entire image and adheres to standards set forth by the scientific community. All reported western blots/immunoblots were repeated in at least biological duplicate.

Benzonase treatment

For Benzonase treatments, we added eight units of Benzonase Nuclease ultrapure (E8263 Sigma) to 0.25 μg BF DNA and four units to 1 μM EVs based on vendor recommendation. Mixture was incubated for 30 min at 37 °C and 5% CO_2 before transfection or stimulation.

ELISA analysis

Macrophages were plated at a concentration of 1.5×10^5 cells ml^{-1} in a 12-well TC-treated plate for IFNβ enzyme-linked immunosorbet assays (ELISAs) and a concentration of 1×10^4 cells ml^{-1} in a 96-well plate for the TNF ELISA. For the IFNβ ELISA, macrophages were either stimulated with PBS, EVs or transfected with cGAMP, or *C. albicans* DNA from BF. Transfections were completed using the Lipofectamine 3000 reagents and protocol (Invitrogen L3000015). Supernatants were collected following a 6 h (IFNβ) and 2 h (TNFα) stimulation at 37 °C and 5% CO_2. IFNβ levels were assessed on these supernatants using ELISA (Duoset, R and D Systems) per the manufacturer's instructions and read using an i3X Spectrophotometer (Molecular Devices, LLC). Results were analysed using PRISM9 software (GraphPad Software). All reported ELISAs were done in both technical and biological triplicate.

Microscopy

cGAS–GFP-expressing macrophages were plated on Nunc Lab-Tek eight-well chambered coverglass (Thermo Fisher Scientific). Macrophages were plated at a concentration of 1×10^5 cells ml^{-1} in 500 μl and incubated overnight (~18 h) at 37 °C and 5% CO_2. For stimulation, 50 μl of EVs (~10^{11}) were either dyed with 5 μM DiI lipophilic stain (Invitrogen D282) or untreated for 30 min at RT. Following staining, EVs were washed twice with PBS, using an ultracentrifuge to pellet the EVs at 100,000*g* for 1 h. A PBS plus DiI sample was also subjected to the same wash steps. Before stimulation, macrophages were washed three times with PBS to remove FBS and any mammalian EVs present from serum. Macrophages were then refreshed with DMEM without FBS and PBS; EVs, DiI-stained EVs or DiI-stained PBS were added to wells. Stimulated cells were then incubated for 3 h at 37 °C and 5% CO_2 to allow phagocytosis of EVs. Images were captured on a Nikon Inverted Microscope Eclipse Ti-E equipped with a CSU-X1 confocal spinning disk head (Yokogawa), and a Coherent 4 W continuous-wave laser (Coherent) excited the sample. A 100× high-numerical aperture objective (Nikon, 1003, 1.49 numerical aperture, oil immersion) was used. Images were obtained using an EMCCD camera (Hamamatsu Photonics). Image acquisition was performed using MetaMorph software (Molecular Devices). Raw images were then cropped by FIJI and assembled in Adobe Illustrator, version CS4 (Adobe Systems). Macrophage cGAS localization was quantified as either nuclear (only nuclear localization), non-nuclear (only cytosolic localization) or mixed (a combination of nuclear and cytosolic).

RNA extraction and NanoString analysis

Macrophages were plated at a concentration of 1.5×10^5 cells ml^{-1} in a 12-well TC-treated plate and incubated overnight (~18 h) at 37 °C and 5% CO_2. Macrophages were either stimulated with PBS, EVs, or transfected with Lipofectamine alone or *C. albicans*

DNA from BFs grown for 72 h. Samples were collected following a 6 h incubation at 37 °C and 5% CO_2. NanoString (nanoString) profiling of transcriptional responses was performed using the nCounter Host Response Panel according to manufacturer's instructions. Gene expression of host response genes was measured via NanoString Technology by first isolating RNA using the QIAGEN RNeasy Mini Kit. RNA was then measured via nanodrop and diluted to 25 ng per reaction. RNA was then hybridized in hybridization buffer at 65 °C for 18 h with the Host Response Gene Panel Reporter Codeset and Capture Probeset (nCounter). Hybridized samples were then loaded into a nCounter Cartridge and analysed using a nCounter Sprint Profiler for 6 h. Data were then normalized and analysed by nSolver. Subsequent heatmaps and graphs were made in nSolver, Prism and BioVenn. Each NanoString experiment was run in biological duplicate. Genes were normalized to the controls included in the plate for each genotype to account for variability, and Supplementary Table 2 includes these normalized ratios. RT–qPCR validation was performed on extracted RNA via Invitrogen EXPRESS One-Step Superscript (11781200). Primers for mouse RSAD2 (4453320, Mm00491265_m1), OASL (4448892, Mm00455081_m1) and IFIT3 (4453320, Mm01704846_s1) were ordered from Thermo Fisher.

Macrophage differentiation and stimulation and cytokine quantitative trait loci mapping

Details of the macrophage differentiation and stimulation experiments, as well as cytokine quantitative trait locus association analysis of the 500FG cohort, have been previously described[83]. Briefly, monocytes were plated at a concentration of $>5 \times 10^5$ in flat-bottom plates with 10% human serum at 37 °C and 5% CO_2 for 6 days. After differentiation, the medium was removed and the differentiated macrophages were stimulated with heat-killed *C. albicans* for 24 h (strain ATCC MYA-3573, UC 820) in a concentration of 10^6 CFU ml^{-1}. Supernatants were collected and stored at −20 °C until ELISA experiments were conducted to measure cytokines concentrations. Concentrations of IL6 and TNFα were profiled in macrophages. To explore the strength of association of genetic polymorphisms in cGAS and TMEM173 genes, we extracted genetic variants using a window size of 250 kb upstream and downstream of each gene, and results were visualized with the LocusZoom tool[84]. The 500FG cohort consists of approximately 500 healthy individuals of European origin with age range of 18–75 years. We queried the most significant or top SNPs for statistical evidence of association with the target genes using the eQTLGen database (https://www.eqtlgen.org/).

Reporting summary

Further information on research design is available in the Nature Portfolio Reporting Summary linked to this article.

Extended Data

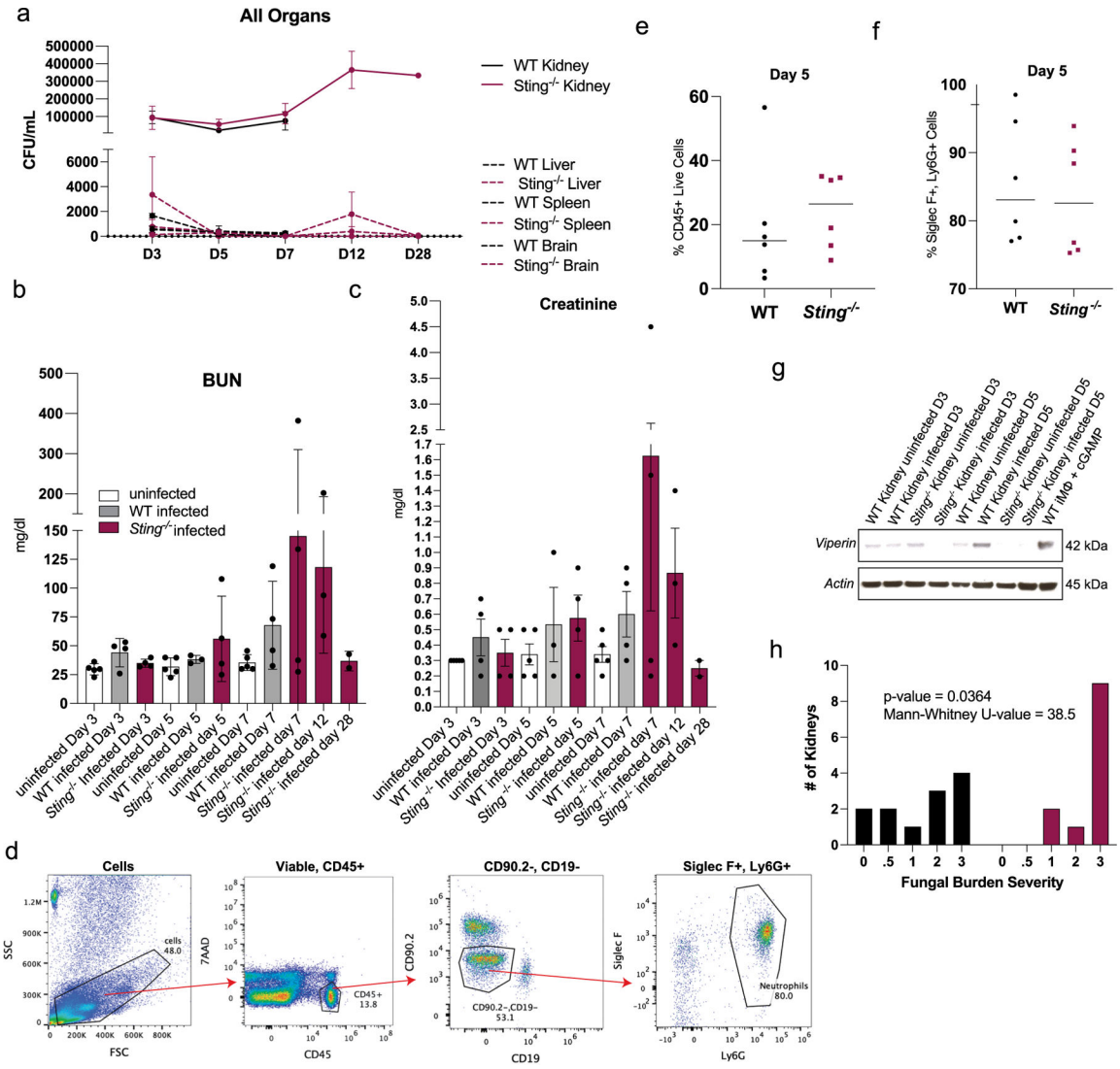

Extended Data Fig. 1 |. Characterization of organs and serum from *C. albicans*-infected WT and *Sting*$^{-/-}$ mice.

a. Quantification of fungal burden following a *C. albicans* infection in WT and *Sting*$^{-/-}$ mice in the kidneys, liver, spleen, and brains (n = 4 for WT and *Sting*$^{-/-}$ for each time point). Kidney BUN **(b)** and creatinine levels **(c)** were measured from serum of infected and uninfected WT and *Sting*$^{-/-}$ mice over 28 days. n = 5 for each time point. **d**. Representative gating strategy for flow cytometry analysis showing selection of total kidney cells (SSC v FSC) → live white blood cells (WBC) (7AAD- and CD45 +) → WBCs that are not B cells or T cells (CD90.2-, CD19-), and of these, how many are neutrophils (Siglec F + , Ly6G +). **e**. Quantification of flow-based immunophenotyping of CD45+ WBCs and **(f)** Siglec F + , Ly6G+ neutrophils from single cell suspensions of kidneys from WT and *Sting*$^{-/-}$ mice (n = 6 for each group). **g**. Immunoblot of viperin from kidney homogenates harvested from WT and *Sting*$^{-/-}$ mice infected with 150,000 *C. albicans* at day 3 and day 5, compared to the positive control (immortalized WT macrophages stimulated with cGAMP for 6 h prior

to lysis). **h**. Semi-quantification of fungal burden severity in GMS-stained kidney sections of WT and *Sting*$^{-/-}$ mice (n = 12). Statistical analyses were performed on raw data by means of a non-parametric, two-tailed Mann Whitney U test = 38.5, $p = 0.0364$. Data are presented as mean values +/− SD.

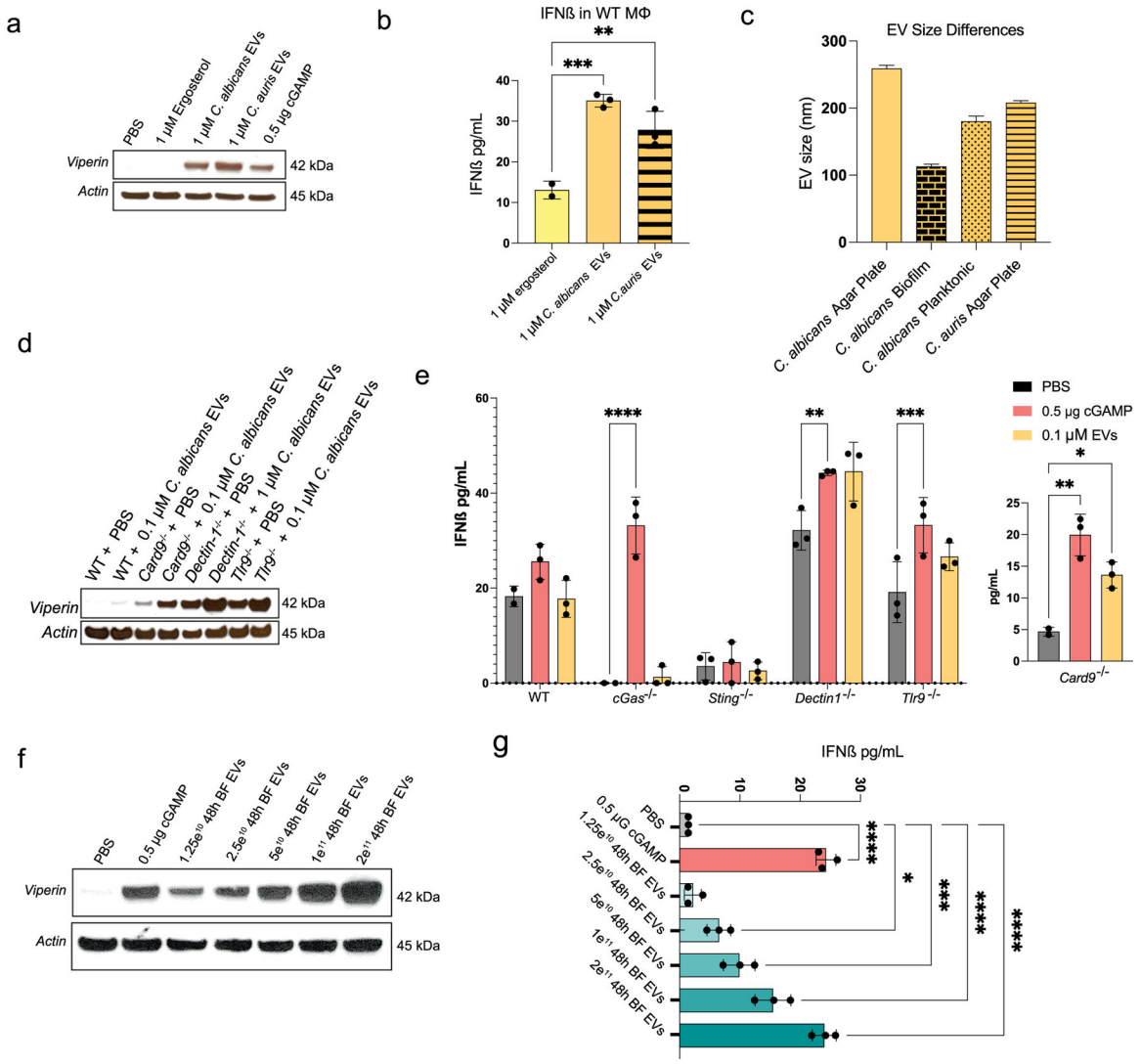

Extended Data Fig. 2 |. Further characterization of the viperin and IFNß response to *C. albicans* EVs.

a. Immunoblot of viperin in lysates from WT macrophages stimulated with PBS, ergosterol alone, EVs from *C. albicans* or *C. auris*, or cGAMP. **b**. IFNß production in the supernatants from the same stimulated WT macrophages as in (a). Significance determined using a one-way ANOVA, ***adj. $p = 0.0004$, **adj. $p = 0.004$ **c**. Average sizes of EVs extracted from *C. albicans* (grown in different conditions) and *C. auris*. **d**. Immunoblot of viperin induction in WT, *Card9*$^{-/-}$, *Dectin-1*$^{-/-}$, and *Tlr9*$^{-/-}$ immortalized macrophages following stimulation with PBS or *C. albicans* EVs. **e**. IFNß production by WT, *cGAS*$^{-/-}$, *Sting*$^{-/-}$, *Card9*$^{-/-}$, *Dectin-1*$^{-/-}$, and *Tlr9*$^{-/-}$ macrophages following a stimulation with PBS, cGAMP, or *C. albicans* EVs. Significance determined using a two-way ANOVA and subsequent

Dunnett's multiple comparison test with the exception of *Card9*$^{-/-}$, which was an ordinary one-way ANOVA and subsequent Dunnett's multiple comparison test, *adj. $p = 0.0031$, **adj. $p < 0.01$, ***adj. $p < 0.001$, ****adj. $p < 0.0001$ vs PBS **f**. Immunoblot of viperin and **g**. IFNß production by WT macrophages stimulated with graded amounts of EVs extracted from *C. albicans* 48 h BF. Significance determined using a one-way ANOVA and subsequent Dunnett's multiple comparison test *adj. $p = 0.0364$, ***adj. $p = 0.0008$, ****adj. $p < 0.0001$ vs PBS. n = 3 biologically independent samples for all ELISAs and data are presented as mean values +/− SD. All Westerns were done in biological triplicate, representative blot shown. Macrophages were stimulated for 6 h prior to processing.

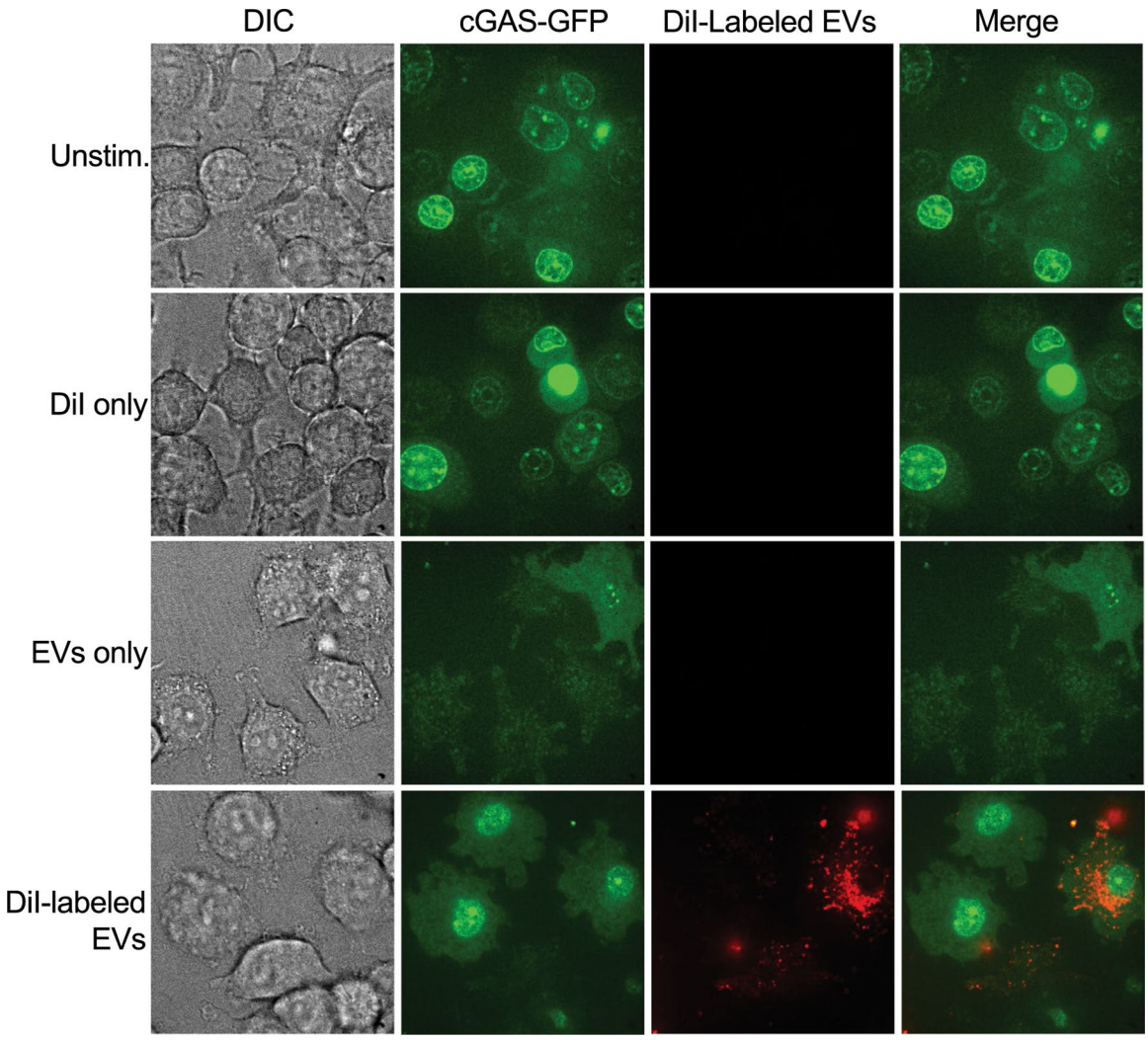

Extended Data Fig. 3 |. *C. albicans* EVs induce translocation of cGAS from the nuclear membrane to the cytosol.

Representative microscopy images of macrophages expressing cGAS-GFP and the localization of cGAS following no stimulation or stimulation with DiI only, *C. albicans* EVs only, or DiI-labeled *C. albicans* EVs. Macrophages were stimulated for 3 h prior to imaging. Size bar = 5 μm. Microscopy experiments were repeated with appropriate controls in biological triplicate, representative images shown of similar results.

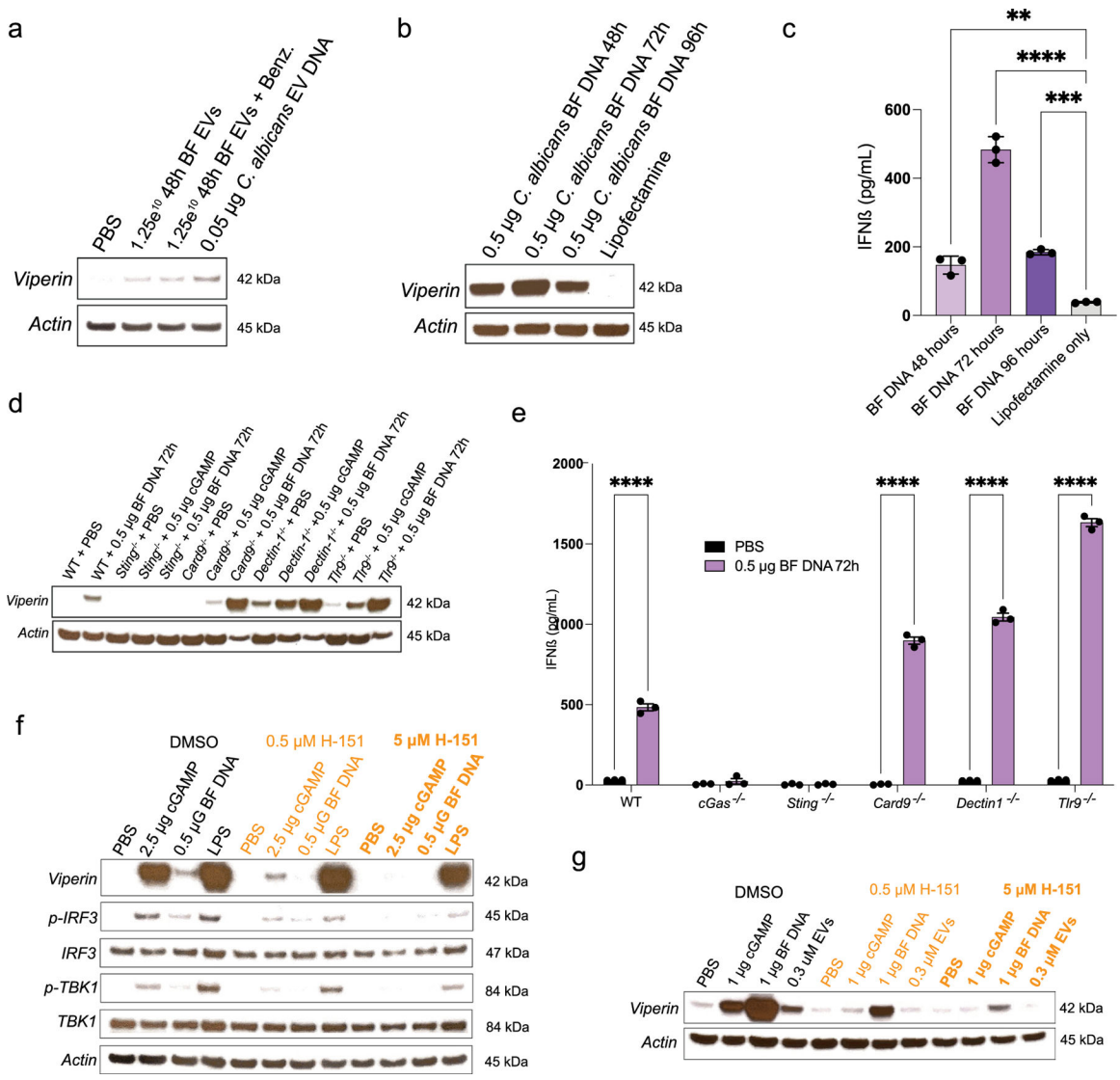

Extended Data Fig. 4 |. Further characterization of the viperin and IFNß response to *C. albicans* BF DNA.

a. Immunoblot of viperin induction in WT macrophages stimulated with PBS, *C. albicans* EVs, Benzonase-treated EVs, and transfected EV DNA. **b**. Immunoblot of viperin induction and **c**. IFNβ production in WT macrophages stimulated with DNA extracted from *C. albicans* biofilms (BF) grown for 48 h, 72 h, 96 h and Lipofectamine reagents only. Significance was determined with an ordinary one-way ANOVA and subsequent Dunnett's multiple comparison test. **adj. $p = 0.0012$, ***adj. $p = 0.0002$, ***adj. $p < 0.0001$ vs untreated control (Lipofectamine). **d**. Immunoblot of viperin induction in WT, *Sting*$^{-/-}$, *Card9*$^{-/-}$, *Dectin-1*$^{-/-}$, and *Tlr9*$^{-/-}$ macrophages following a stimulation with PBS, cGAMP, and DNA extracted from *C. albicans* BF grown for 72 h. **e**. IFNß production by WT, *cGas*$^{-/-}$, *Sting*$^{-/-}$, *Card9*$^{-/-}$, *Dectin-1*$^{-/-}$, and *Tlr9*$^{-/-}$ macrophages following a stimulation with PBS and DNA extracted from *C. albicans* BF grown for 72 h. Significance determined using a two-way ANOVA and subsequent Dunnett's multiple comparison test. ****$p < 0.0001$ vs untreated control (PBS). **f**. Immunoblot of STING pathway component in WT, *cGas*$^{-/-}$, and

Sting$^{-/-}$ immortalized macrophages treated with increasing concentrations of the STING inhibitor, H-151. Cells were treated with H-151 1 h prior to stimulation with PBS, cGAMP, *C. albicans* BF DNA, or LPS (STING independent positive control). **g**. Immunoblot of viperin and actin in WT, *cGas*$^{-/-}$, and *Sting*$^{-/-}$ macrophages treated with the H-151 1 h prior to PBS, cGAMP, *C. albicans* BF DNA, or *C. albicans* EV stimulation. All macrophages were stimulated for 6 h prior to processing. n = 3 biologically independent samples for all ELISAs and data are presented as mean values +/− SD. All Westerns were done in biological triplicate, representative blot shown.

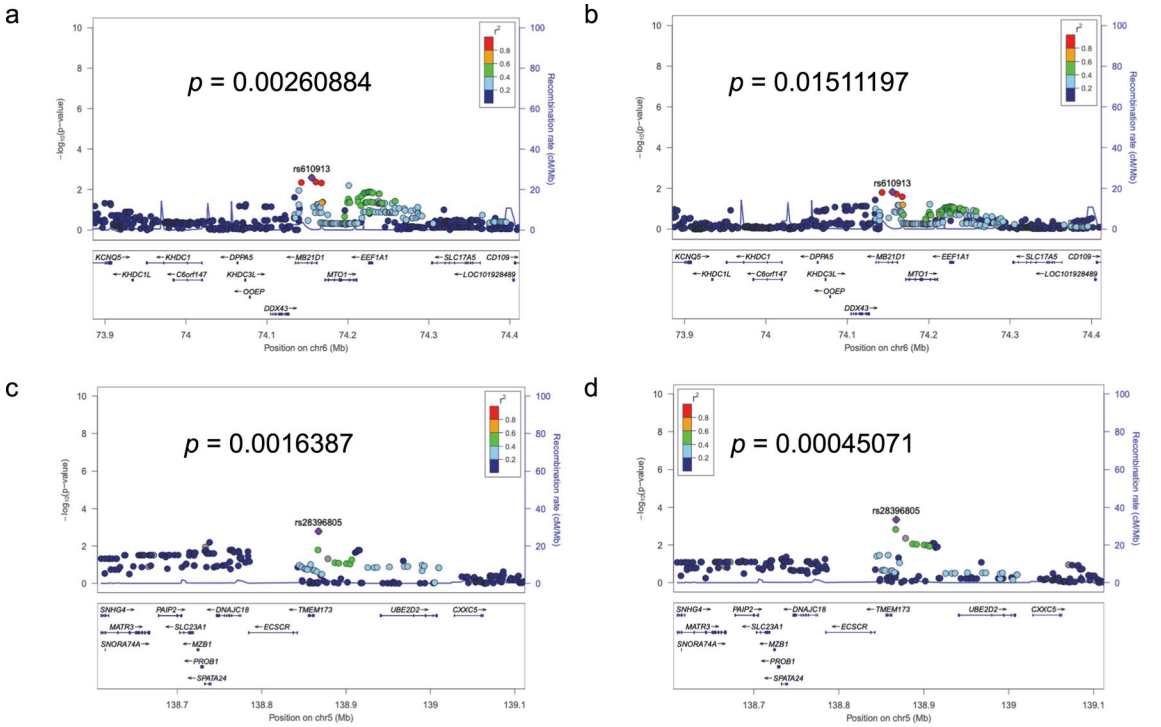

e

P-value	ID	Chr	Pos (hg19)	ID	Symbol	Chr	Pos (hg19)	Z-score	Assessed	Other
7.06E-105	rs610913	6	74155346	ENSG00000164430	MB21D1	6	74142618	-21.7489	G	T
3.33E-23	rs28396805	5	138867439	ENSG00000184584	TMEM173	5	138858819	9.9225	C	T

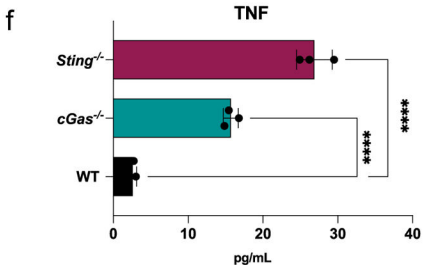

Extended Data Fig. 5 |. Regional association plots for SNPs identified in cGAS and STING. Regional association plot of SNPs around the MB21D1gene locus for *Candida*-induced TNF–α concentrations (**a**) and for *Candida*-induced IL-6 concentrations (**b**). Regional association plot of SNPs around the TMEM173 gene locus for *Candida*-induced TNF–α concentrations (**c**) and for *Candida*-induced IL-6 concentrations (**d**). The -log10 p-values of imputed SNPs are plotted on the y-axis against their physical position (NCBI build 36) on

the x-axis. The most strongly associated SNPs in the regions are represented with purple diamond and surrounding markers are color coded according to their correlation coefficient (r^2) with the top SNP using the hg19/1000 Genomes European samples. The light blue lines denote the estimated recombination rates. **e**. Evidence of the top SNPs regulation the expression levels of *MB21D1* and *TMEM173*. We queried the most significant or top SNPs for statistical evidence of association with the target genes using the eQTLGen database and considered a p value of $< 5 \times 10^{-8}$ to be the threshold for significant cytokine QTLs. **f**. TNF production by WT, *cGas*$^{-/-}$, and *Sting*$^{-/-}$ murine macrophages following a 2 h co-culture with live *C. albicans*. ****adj. $p < 0.0001$ vs. WT. n = 3 biologically independent samples for ELISA and data are presented as mean values +/− SD. Significance determined using an ordinary one-way ANOVA and subsequent Dunnett's multiple comparison test.

Supplementary Material

Refer to Web version on PubMed Central for supplementary material.

Acknowledgements

We thank all the members of the Vyas and Mansour lab at MGH for useful discussions and reading of the paper. We thank K. Timmer for his expert assistance with all flow cytometry experiments. Financial support: H.B.H. is supported by the Fund for Medical Discovery Fellowship from MGH. J.M.V. is supported by R01AI150181, R01AI136529 and R21AI152499; J.L.R. is supported by NIH/NIAID grant 1K08AI14755; D.R.A. is supported by R01AI073289; R.P.B. is supported by R01AI153405; J.E.N. is supported by R21AI159583 and R01AI145939; J.C.K. is supported by R01AI167993 and R37AI116550; and J.D.N. is supported by R21AI156104.

Data availability

The datasets generated during and/or analysed during the current study are available from the corresponding author on reasonable request. Source data are provided with this paper.

References

1. Tsay S et al. National burden of candidemia, United States, 2017. Open Forum Infect. Dis 5, S142 (2018).
2. Cornely OA et al. Epidemiology and outcome of fungemia in a cancer Cohort Of the Infectious Diseases Group (IDG) of the European Organization for Research and Treatment of Cancer (EORTC 65031). Clin. Infect. Dis 10.1093/cid/civ293 (2015).
3. Smeekens SP et al. Functional genomics identifies type I interferon pathway as central for host defense against Candida albicans. Nat. Commun 4, 1342 (2013). [PubMed: 23299892]
4. Pekmezovic M et al. Candida pathogens induce protective mitochondria-associated type I interferon signalling and a damage-driven response in vaginal epithelial cells. Nat. Microbiol 6, 643–657 (2021). [PubMed: 33753919]
5. Bourgeois C et al. Conventional dendritic cells mount a type I IFN response against Candida spp. Requiring novel phagosomal TLR7-mediated IFN-β signaling. J. Immunol 186, 3104–3112 (2011). [PubMed: 21282509]
6. delFresno C et al. Interferon-β production via Dectin-1-Syk-IRF5 signaling in dendritic cells is crucial for immunity to C. albicans. Immunity 38, 1176–1186 (2013). [PubMed: 23770228]
7. Jaeger M et al. The RIG-I-like helicase receptor MDA5 (IFIH1) is involved in the host defense against Candida infections. Eur. J. Clin. Microbiol. Infect. Dis 34, 963 (2015). [PubMed: 25579795]
8. Ishikawa H & Barber GN STING is an endoplasmic reticulum adaptor that facilitates innate immune signalling. Nature 455, 674–678 (2008). [PubMed: 18724357]

9. Decout A, Katz JD, Venkatraman S & Ablasser A The cGAS–STING pathway as a therapeutic target in inflammatory diseases. Nat. Rev. Immunol 21, 548–569 (2021). [PubMed: 33833439]
10. Chen T et al. The nucleotide receptor STING translocates to the phagosomes to negatively regulate anti-fungal immunity. Immunity 56, 1727–1742.e6 (2023). [PubMed: 37379835]
11. Sun L, Wu J, Du F, Chen X & Chen ZJ Cyclic GMP–AMP synthase is a cytosolic DNA sensor that activates the type I interferon pathway. Science 339, 786–791 (2013). [PubMed: 23258413]
12. Diner EJ et al. The innate immune DNA sensor cGAS produces a noncanonical cyclic dinucleotide that activates human STING. Cell Rep 3, 1355–1361 (2013). [PubMed: 23707065]
13. Ablasser A et al. cGAS produces a 2′-5′-linked cyclic dinucleotide second messenger that activates STING. Nature 498, 380–384 (2013). [PubMed: 23722158]
14. Fischer K et al. Cutibacterium acnes infection induces type I interferon synthesis through the cGAS–STING pathway. Front. Immunol 11, 2630 (2020).
15. McNab F, Mayer-Barber K, Sher A, Wack A & O'Garra A Type I interferons in infectious disease. Nat. Rev. Immunol 15, 87–103 (2015). [PubMed: 25614319]
16. Hansen K et al. Listeria monocytogenes induces IFNβ expression through an IFI16-, cGAS- and STING-dependent pathway. EMBO J 33, 1654–1666 (2014). [PubMed: 24970844]
17. Neufeldt CJ et al. SARS-CoV-2 infection induces a pro-inflammatory cytokine response through cGAS–STING and NF-κB. Commun. Biol 5, 1–15 (2022). [PubMed: 34987157]
18. Iampietro M et al. Activation of cGAS/STING pathway upon paramyxovirus infection. iScience 24, 102519 (2021). [PubMed: 34142033]
19. Zhang C et al. Structural basis of STING binding with and phosphorylation by TBK1. Nature 567, 394–398 (2019). [PubMed: 30842653]
20. Vargas G et al. Compositional and immunobiological analyses ofextracellular vesicles released by Candida albicans. Cell. Microbiol 17, 389–407 (2015). [PubMed: 25287304]
21. Zarnowski R et al. Coordination of fungal biofilm development by extracellular vesicle cargo. Nat. Commun. 2021 121 12, 6235 (2021).
22. Zarnowski R et al. A common vesicle proteome drives fungal biofilm development. Proc. Natl Acad. Sci. USA 119, e2211424119 (2022). [PubMed: 36095193]
23. Zamith-Miranda D et al. Comparative molecular and immunoregulatory analysis of extracellular vesicles from Candida albicans and Candida auris. mSystems 6, e0082221 (2021). [PubMed: 34427507]
24. Zarnowski R et al. Candida albicans biofilm-induced vesicles confer drug resistance through matrix biogenesis. PLoS Biol 16, e2006872 (2018). [PubMed: 30296253]
25. Erttmann SF et al. The gut microbiota prime systemic antiviral immunity via the cGAS–STING–IFN-I axis. Immunity 55, 847–861. e10 (2022). [PubMed: 35545033]
26. Reedy JL et al. The C-type lectin receptor Dectin-2 is a receptor for Aspergillus fumigatus Galactomannan. MBio 14, e0318422 (2023). [PubMed: 36598192]
27. Wiesner DL et al. Club cell TRPV4 serves as a damage sensor driving lung allergic inflammation. Cell Host Microbe 27, 614–628. e6 (2020). [PubMed: 32130954]
28. Chin KC & Cresswell P Viperin (cig5), an IFN-inducible antiviral protein directly induced by human cytomegalovirus. Proc. Natl Acad. Sci. USA 98, 15125–15130 (2001). [PubMed: 11752458]
29. Kasperkovitz PV et al. Toll-like receptor 9 modulates macrophage antifungal effector function during innate recognition of Candida albicans and Saccharomyces cerevisiae. Infect. Immun 79, 4858–4867 (2011). [PubMed: 21947771]
30. Gantner BN, Simmons RM & Underhill DM Dectin-1 mediates macrophage recognition of Candida albicans yeast but not filaments. EMBO J 24, 1277 (2005). [PubMed: 15729357]
31. Brown GD & Gordon S Immune recognition. A new receptor for beta-glucans. Nature 413, 36–37 (2001).
32. Civril F et al. Structural mechanism of cytosolic DNA sensing by cGAS. Nature 498, 332–337 (2013). [PubMed: 23722159]
33. Sun H et al. A nuclear export signal is required for cGAS to sense cytosolic DNA. Cell Rep 34, 108586 (2021). [PubMed: 33406424]

34. Volkman HE, Cambier S, Gray EE & Stetson DB Tight nuclear tethering of cGAS is essential for preventing autoreactivity. Elife 8, e47491 (2019). [PubMed: 31808743]
35. Mosallanejad K et al. Three functionally distinct classes of cGAS proteins in nature revealed by self-DNA-induced interferon responses. Preprint at bioRxiv 10.1101/2022.03.09.483681 (2022).
36. Moreno JM, Sanchez-Montero JM, Sinisterra JV & Nielsen LB Contribution to the study of the enzymatic activity of Benzonase. J. Mol. Catal 69, 419–427 (1991).
37. Rajendran R et al. Extracellular DNA release confers heterogeneity in Candida albicans biofilm formation. BMC Microbiol 14, 303 (2014). [PubMed: 25476750]
38. Martins M et al. Presence of extracellular DNA in the Candida albicans biofilm matrix and its contribution to biofilms. Mycopathologia 169, 323–331 (2010). [PubMed: 20012895]
39. Haag SM et al. Targeting STING with covalent small-molecule inhibitors. Nature 559, 269–273 (2018). [PubMed: 29973723]
40. Gulen MF et al. cGAS–STING drives ageing-related inflammation and neurodegeneration. Nature 620, 374–380 (2023). [PubMed: 37532932]
41. Dog S et al. Single-cell analysis of early antiviral gene expression reveals a determinant of stochastic IFNB1 expression. Integr. Biol 9, 857 (2017).
42. Fernandes-Alnemri T, Yu JW, Datta P, Wu J & Alnemri ES AIM2 activates the inflammasome and cell death in response to cytoplasmic DNA. Nature 458, 509–513 (2009). [PubMed: 19158676]
43. Hornung V et al. AIM2 recognizes cytosolic dsDNA and forms a caspase-1-activating inflammasome with ASC. Nature 458, 514–518 (2009). [PubMed: 19158675]
44. Bürckstümmer T et al. An orthogonal proteomic-genomic screen identifies AIM2 as a cytoplasmic DNA sensor for the inflammasome. Nat. Immunol 10, 266–272 (2009). [PubMed: 19158679]
45. Motwani M, Pesiridis S & Fitzgerald KA DNA sensing by the cGAS–STING pathway in health and disease. Nat. Rev. Genet. 2019 2011 20, 657–674 (2019).
46. Stawowczyk M et al. Pathogenic effects of IFIT2 and interferon-β during fatal systemic Candida albicans infection. mBio 9, e00365–18 (2018). [PubMed: 29666281]
47. Zarnowski R et al. Coordination of fungal biofilm development by extracellular vesicle cargo. Nat. Commun 12, 6235 (2021). [PubMed: 34716343]
48. Bitencourt TA et al. Fungal extracellular vesicles are involved in intraspecies intracellular communication. mBio 13, e0327221 (2022). [PubMed: 35012355]
49. Honorato L et al. Extracellular vesicles regulate biofilm formation and yeast-to-hypha differentiation in Candida albicans. mBio 13, e0030122 (2022). [PubMed: 35420476]
50. Mathieu M, Martin-Jaular L, Lavieu G & Théry C Specificities of secretion and uptake of exosomes and other extracellular vesicles for cell-to-cell communication. Nat. Cell Biol 21, 9–17 (2019). [PubMed: 30602770]
51. Raposo G et al. B lymphocytes secrete antigen-presenting vesicles. J. Exp. Med 183, 1161–1172 (1996). [PubMed: 8642258]
52. Valadi H et al. Exosome-mediated transfer of mRNAs and microRNAs is a novel mechanism of genetic exchange between cells. Nat. Cell Biol 9, 654–659 (2007). [PubMed: 17486113]
53. Kanada M et al. Differential fates of biomolecules delivered to target cells via extracellular vesicles. Proc. Natl Acad. Sci. USA 112, 201418401 (2015).
54. Mack M et al. Transfer of the chemokine receptor CCR5 between cells by membrane-derived microparticles: a mechanism for cellular human immunodeficiency virus 1 infection. Nat. Med 6, 769–775 (2000). [PubMed: 10888925]
55. Bonsergent E et al. Quantitative characterization of extracellular vesicle uptake and content delivery within mammalian cells. Nat. Commun 12, 1–11 (2021). [PubMed: 33397941]
56. Balaj L et al. Tumour microvesicles contain retrotransposon elements and amplified oncogene sequences. Nat. Commun 2, 180 (2011). [PubMed: 21285958]
57. Skog J et al. Glioblastoma microvesicles transport RNA and proteins that promote tumour growth and provide diagnostic biomarkers. Nat. Cell Biol 10, 1470–1476 (2008). [PubMed: 19011622]
58. Al-Nedawi K et al. Intercellular transfer of the oncogenic receptor EGFRvIII by microvesicles derived from tumour cells. Nat. Cell Biol 10, 619–624 (2008). [PubMed: 18425114]

59. Coakley G et al. Extracellular vesicles from a helminth parasite suppress macrophage activation and constitute an effective vaccine for protective immunity. Cell Rep 19, 1545–1557 (2017). [PubMed: 28538175]
60. Gomes MTR et al. STING regulates metabolic reprogramming in macrophages via HIF-1α during Brucella infection. PLoS Pathog 17, e1009597 (2021). [PubMed: 33989349]
61. Zhang H, Zoued A, Liu X, Sit B & Waldora MK Type I interferon remodels lysosome function and modifies intestinal epithelial defense. Proc. Natl Acad. Sci. USA 117, 29862–29871 (2020). [PubMed: 33172989]
62. Netea MG, Brown GD, Kullberg BJ & Gow NAR An integrated model of the recognition of Candida albicans by the innate immune system. Nat. Rev. Microbiol 6, 67–78 (2008). [PubMed: 18079743]
63. Nahum A, Dadi H, Bates A & Roifman CM The L412F variant of Toll-like receptor 3 (TLR3) is associated with cutaneous candidiasis, increased susceptibility to cytomegalovirus, and autoimmunity. J. Allergy Clin. Immunol 127, 528–531 (2011). [PubMed: 21093032]
64. Ferwerda G, Meyer-Wentrup F, Kullberg BJ, Netea MG & Adema GJ Dectin-1 synergizes with TLR2 and TLR4 for cytokine production in human primary monocytes and macrophages. Cell. Microbiol 10, 2058–2066 (2008). [PubMed: 18549457]
65. Wagener J et al. Fungal chitin dampens inflammation through IL-10 induction mediated by NOD2 and TLR9 activation. PLoS Pathog 10, e1004050 (2014). [PubMed: 24722226]
66. Hise AG et al. An essential role for the NLRP3 inflammasome in host defense against the human fungal pathogen Candida albicans. Cell Host Microbe 5, 487–497 (2009). [PubMed: 19454352]
67. Pietrella D et al. Secreted aspartic proteases of Candida albicans activate the NLRP3 inflammasome. Eur. J. Immunol 43, 679–692 (2013). [PubMed: 23280543]
68. Majer O et al. Type I interferons promote fatal immunopathology by regulating inflammatory monocytes and neutrophils during Candida infections. PLoS Pathog 8, e1002811 (2012). [PubMed: 22911155]
69. Kolben T et al. IL-23, IFN-α, and IFN-β in the vaginal fluid of patients suffering from vulvovaginal candidosis. Clin. Exp. Obstet. Gynecol 44, 7–10 (2017). [PubMed: 29714856]
70. Biondo C et al. Recognition of yeast nucleic acids triggers a host-protective type I interferon response. Eur. J. Immunol 41, 1969–1979 (2011). [PubMed: 21480215]
71. Han F et al. The cGAS-STING signaling pathway contributes to the inflammatory response and autophagy in Aspergillus fumigatus keratitis. Exp. Eye Res 202, 108366 (2021). [PubMed: 33227296]
72. Souza JAM et al. Characterization of Aspergillus fumigatus extracellular vesicles and their effects on macrophages and neutrophils functions. Front. Microbiol 10, 2008 (2019). [PubMed: 31551957]
73. Rizzo J et al. Characterization of extracellular vesicles produced by Aspergillus fumigatus protoplasts. mSphere 10.1128/msphere.00476-20 (2020).
74. Dutta O, Espinosa V, Wang K, Avina S & Rivera A Dectin-1 promotes type I and III interferon expression to support optimal antifungal immunity in the lung. Front. Cell Infect. Microbiol 10, 321 (2020). [PubMed: 32733815]
75. Espinosa V et al. Type III interferon is a critical regulator of innate antifungal immunity. Sci. Immunol 2, eaan5357 (2017). [PubMed: 28986419]
76. Jiang GL et al. cGAS knockdown promotes microglial M2 polarization to alleviate neuroinflammation by inhibiting cGAS-STING signaling pathway in cerebral ischemic stroke. Brain Res. Bull 171, 183–195 (2021). [PubMed: 33745949]
77. Tam JM et al. Tetraspanin CD82 organizes Dectin-1 into signaling domains to mediate cellular responses to Candida albicans. J. Immunol 202, 3256–3266 (2019). [PubMed: 31010852]
78. Gray EE, Treuting PM, Woodward JJ & Stetson DB Cutting edge: cGAS is required for lethal autoimmune disease in the Trex1-deficient mouse model of Aicardi–Goutières syndrome. J. Immunol 195, 1939–1943 (2015). [PubMed: 26223655]
79. Barnett KC et al. Phosphoinositide interactions position cGAS at the plasma membrane to ensure efficient distinction between self- and viral DNA. Cell 176, 1432–1446.e11 (2019). [PubMed: 30827685]

80. Kasperkovitz PV, Cardenas ML & Vyas JM TLR9 Is actively recruited to Aspergillus fumigatus phagosomes and requires the N-terminal proteolytic cleavage domain for proper intracellular trafficking. J. Immunol 185, 7614–7622 (2010). [PubMed: 21059889]

81. Zamith-Miranda D, Alves LR, Rodrigues ML, Nimrichter L & Nosanchuk JD Isolation of extracellular vesicles from Candida auris. Methods Mol. Biol 2517, 173–178 (2022). [PubMed: 35674953]

82. Zarnowski R, Sanchez H & Andes DR Large-scale production and isolation of Candida biofilm extracellular matrix. Nat. Protoc 11, 2320–2327 (2016). [PubMed: 27809313]

83. Li Y et al. A functional genomics approach to understand variation in cytokine production in humans. Cell 167, 1099–1110.e14 (2016). [PubMed: 27814507]

84. Pruim RJ et al. LocusZoom: regional visualization of genome-wide association scan results. Bioinformatics 26, 2336–2337 (2010). [PubMed: 20634204]

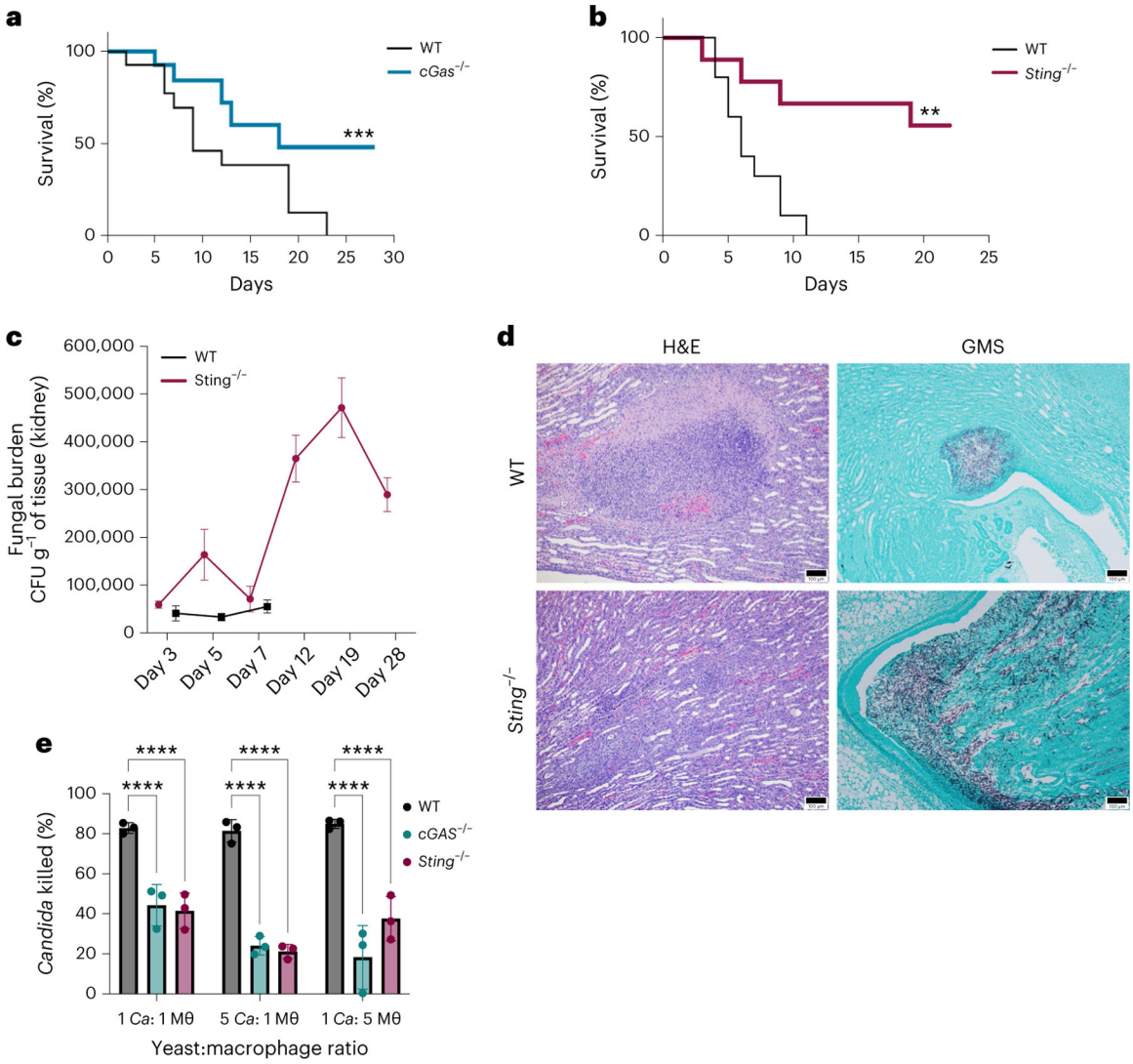

Fig. 1 |. Deletion of cGAS or STING renders mice more resistant to intravenous *C. albicans*.
a,**b**, WT, *cGas*$^{-/-}$ (**a**), and *Sting*$^{-/-}$ (**b**) mice were infected intravenously with 100,000 or 150,000 *C. albicans* yeast, respectively. The data are presented as Kaplan–Meier survival curves representative of three experiments ($n = 14$ for each group, and significance was determined using a log-rank test (Mantel–Cox) $^{**}P = 0.0041$, $^{***}P < 0.001$ versus WT, data are presented as mean values ± standard deviation). **c**, Quantification of renal fungal burden following a *C. albicans* infection in WT and *Sting*$^{-/-}$ mice ($n = 8$ for WT and 14 for *Sting*$^{-/-}$ for each timepoint). **d**, Histological analysis of kidney sections from WT and *Sting*$^{-/-}$ mice at day 5 following a *C. albicans* infection. Host immune cells and fungal cells were identified by H&E and GMS staining, respectively. Scale bar, 100 μm. **e**, Efficacy of fungal killing by WT, *cGas*$^{-/-}$ and *Sting*$^{-/-}$ immortalized macrophages to kill *C. albicans* for 2 h at varying ratios. Data calculated by two-way ANOVA and subsequent Dunnett's multiple comparison test. Data are presented as mean values from three biological replicates ± standard deviation, $^{****}P < 0.0001$ versus WT.

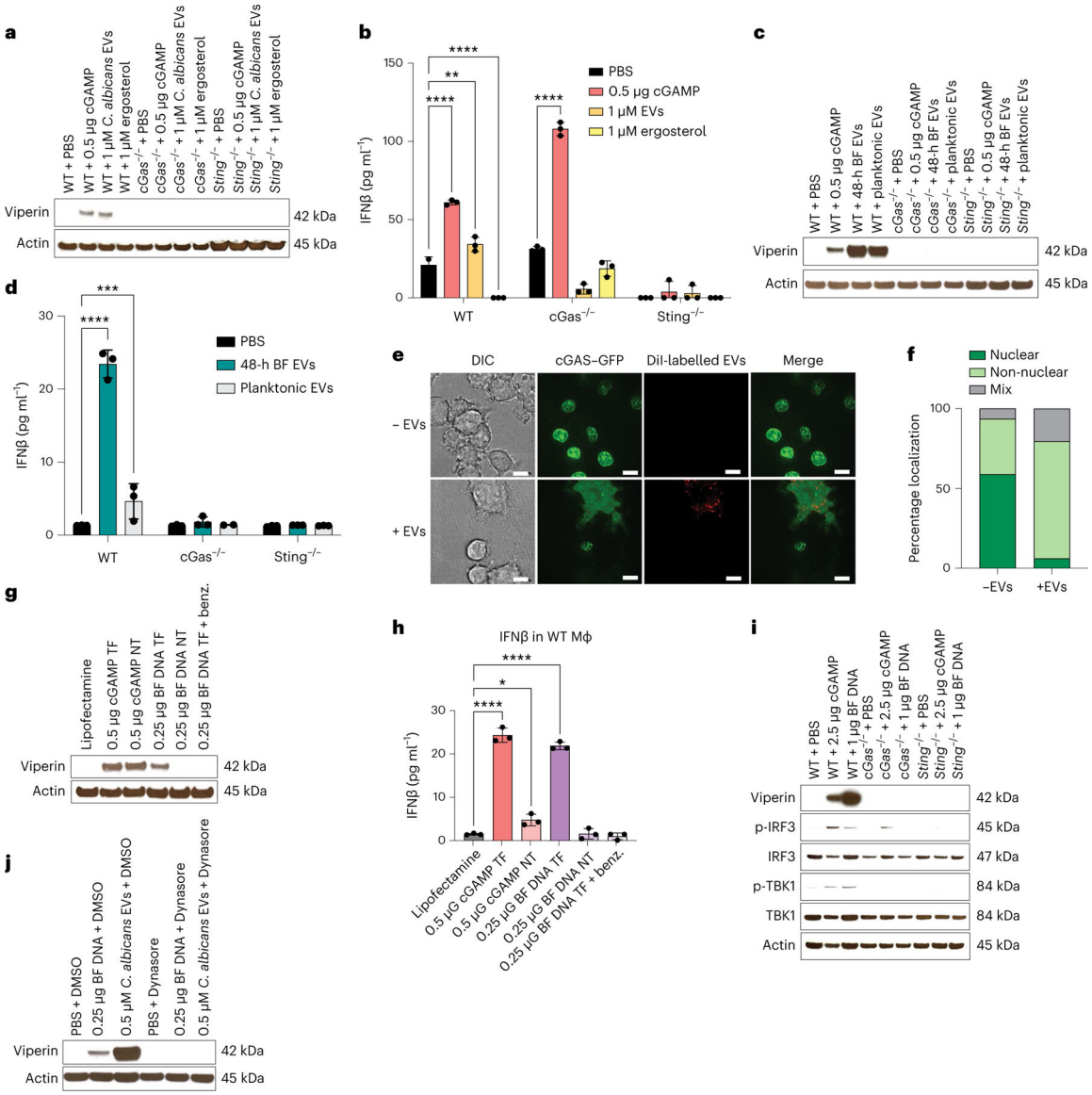

Fig. 2 |. *C. albicans* EVs and BF DNA activate the STING pathway.

a, Immunoblot of viperin in WT, *cGAS*$^{-/-}$ and *Sting*$^{-/-}$ macrophages in response to PBS, cGAMP, *C. albicans* EVs or ergosterol. **b**, Secretion of IFNβ by WT, *cGas*$^{-/-}$ and *Sting*$^{-/-}$ macrophages stimulated with PBS, cGAMP, *C. albicans* EVs and ergosterol. **c**, Immunoblot of viperin induction in WT, *cGAS*$^{-/-}$ and *Sting*$^{-/-}$ macrophages following a stimulation with PBS, cGAMP and EVs extracted from either *C. albicans* BF grown for 48 h or *C. albicans* planktonic culture. **d**, IFNβ production by WT, *cGas*$^{-/-}$ and *Sting*$^{-/-}$ macrophages, following a stimulation with PBS, EVs extracted from either a *C. albicans* BF grown for 48 h, or *C. albicans* planktonic culture. **e**. Representative microscopy images of cGAS–GFP macrophages with and without stimulation with DiI-labelled *C. albicans* BF EVs (DIC = differential interference contrast). Macrophages were stimulated for 3 h before imaging. **f**. Quantification of nuclear versus non-nuclear cGAS–GFP localization patterns in unstimulated and stimulated cells. **g**,**h**, Immunoblot of viperin (**g**) and IFNβ

production in response to non-transfected (NT) and transfected (TF) cGAMP, BF DNA and Benzonase (Benz.)-treated BF DNA (**h**). **i**, Immunoblot of phosphorylated IRF3, total IRF3, phosphorylated TBK1, total TBK1 and actin in response to TF cGAMP and BF DNA in WT, *cGas*$^{-/-}$ and *Sting*$^{-/-}$ macrophages. **j**, Immunoblot of viperin in WT cells treated with Dynasore or vehicle control of dimethyl sulfoxide (DMSO) before stimulation with PBS, *C. albicans* EVs and TF *C. albicans* BF DNA. Macrophages were stimulated for 6 h before processing. Two-way (**b** and **d**) and one-way (**h**) ANOVAs with subsequent Dunnett's multiple comparison tests are shown for ELISAs. Data are presented as mean values from three biological triplicates ± standard deviation, with adjusted (adj.) *P* values. *adj. $P = 0.0143$, **adj. $P = 0.012$, ***adj. $P = 0.0007$, ****adj. $P < 0.0001$ versus untreated control (PBS or Lipofectamine). All western blots were done in biological triplicate, representative blot shown.

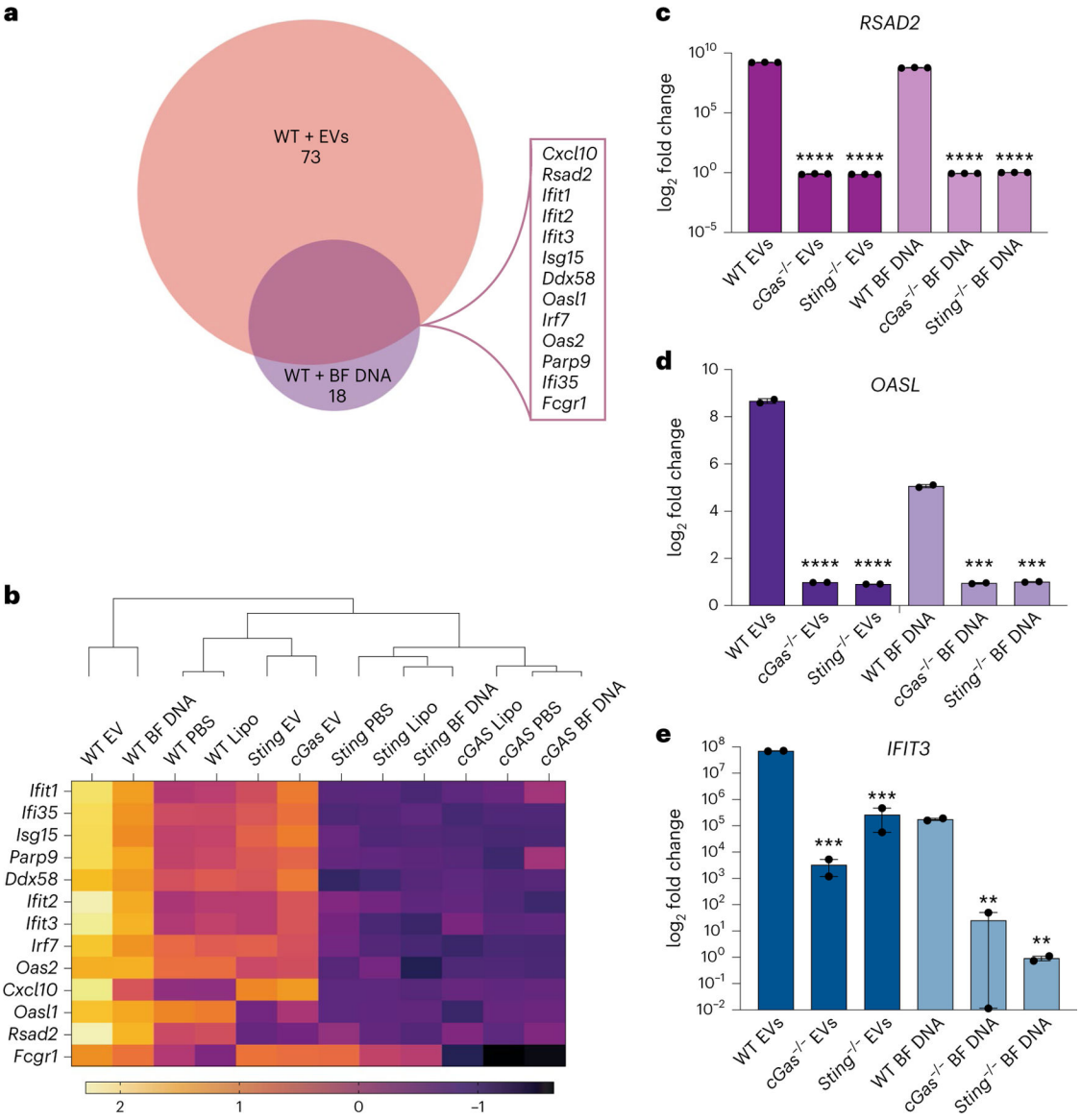

Fig. 3 |. Early ISG upregulation in WT macrophages stimulated by *C. albicans* EVs and BF DNA.

a, Venn diagram of genes identified by NanoString analysis as induced by *C. albicans* EVs and BF DNA in WT macrophages as compared with their controls (PBS and Lipofectamine alone, respectively). The 13 overlapping genes are highlighted in the purple box and the ISGs are bolded. **b**, A heatmap is shown of normalized counts with *z*-scores and unsupervised clustering of these 13 overlapping genes in WT, *cGas*$^{-/-}$ and *Sting*$^{-/-}$ macrophages stimulated with PBS EVs, BF DNA or Lipofectamine (Lipo) alone. **c**–**e**, RT–qPCR analysis of *RSAD2* (**c**), *OASL* (**d**) and *IFIT3* (**e**) in WT, *cGas*$^{-/-}$ and *Sting*$^{-/-}$ macrophages after stimulation with PBS, EVs, Lipofectamine or BF DNA is shown, $n = 3$. All data are representative of at least two independent experiments. For RT–qPCR panels, error bars indicate the standard deviation, and statistical analyses were performed by means of unpaired two-tailed Student's *t*-tests as compared with the appropriate control, with $^{**}P < 0.01$; $^{***}P = 0.0002$; and $^{****}P < 0.0001$.

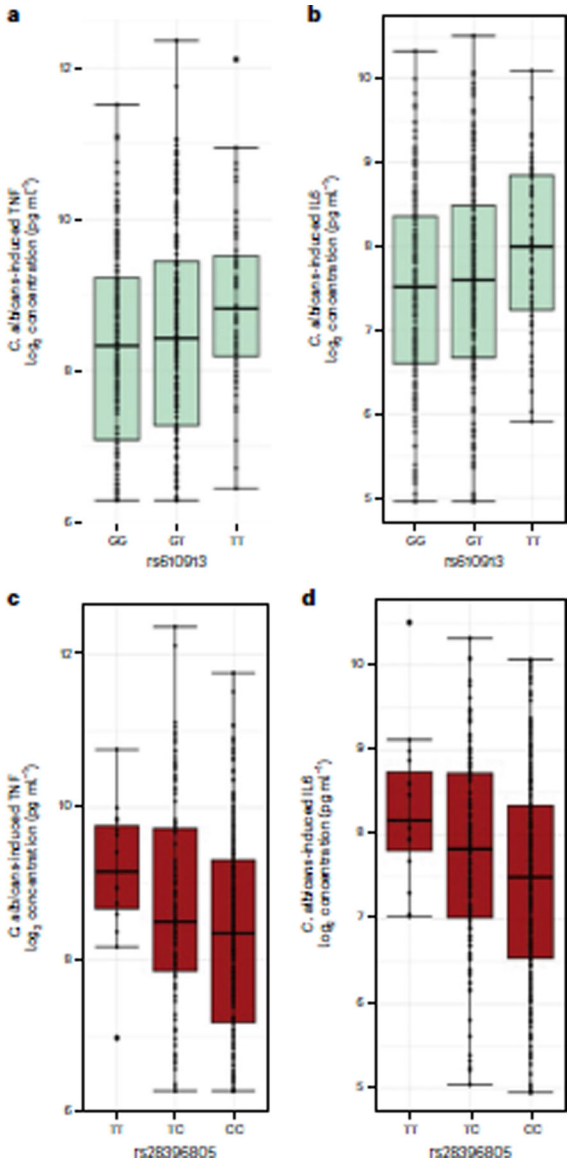

Fig. 4 |. Functional consequence of activating the STING pathway.

a,**b**, Boxplots show the top SNP rs610913 at the MB21D1 locus (*cGAS*) stratified by genotypes for *C. albicans*-induced TNFα concentrations (**a**) and for *C. albicans*-induced IL6 concentrations (**b**). **c**,**d**, Individuals homozygous for the G allele (GG) on average produce less TNFα and IL6 than individuals carrying one G allele (GT) or homozygous for the T allele (TT). Boxplots show the top SNP rs28396805 at the TMEM173 locus (*STING*) stratified by genotypes for *C. albicans*-induced IL6 concentrations (**c**) and *C. albicans*-induced TNFα concentrations (**d**). On average, carriers of the C allele (CC and TC) produce less IL6 and TNFα than individuals homozygous for the T allele (TT). The minimum portion of the error bars denote the first quartile (25th percentile) and the maximum part of the error bars represent the third quartile (75th percentile). The black line in the middle denotes the median (50th) percentile. The black dots are whiskers that span

between the minimum and maximum values. A total of $n = 442$ samples have genotype and cytokine data from the 500FG cohort[83].